ESR of Copper and Iron Complexes with Antitumor and Cytotoxic Properties

by William E. Antholine,* Balaraman Kalyanaraman,* and David H. Petering†‡

The relatively few iron and copper metal complexes which have been examined in cells and tissues for their redox properties, radical generation properties, and antitumor activity are discussed for studies which utilized electron spin resonance spectroscopy (ESR). A common property of a number of metal complexes, which include bleomycin, adriamycin, and thiosemicarbazones described in this review, is that they are readily reduced by thiol compounds and oxidized by oxygen or reduced species of oxygen to produce radicals. Structural features of these reactions are identified by ESR spectroscopy in model systems and often in cells. Furthermore, ESR spectroscopy has been most useful to probe the environment of the complexes in cells and to measure the rate of reduction of their oxidized forms. As a result of these studies, it is anticipated that more attention will be given to the exploration of redox-active metal complexes as drugs.
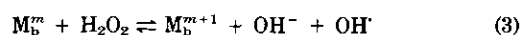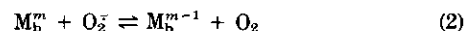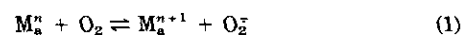
Introduction

It has long been known that the interaction of radiation with cells and tissues is a complicated process beginning with the cleavage of H_2O into e^-, $H\cdot$, or $OH\cdot$ radicals. These radical species then react indiscriminately with cellular constituents. The cytotoxic reactions are thought to involve radical attack on DNA (1–3). The extent of radiation damage to tissues can be modified by modulation of their oxygen and thiol content.

An analogous hypothesis exists for damage to tissues and cells caused by radicals which are generated by photolysis or redox chemistry which often involves a metal ion instead of high energy radiation. While other papers in this issue center on the detection of radicals, this paper focuses on metal complexes which can be catalysts for generation of the more visible radicals and radical damage. Moreover, this review is limited to a description of those metal complexes which can be detected by electron spin resonance spectroscopy (ESR). ESR only detects metal ions with unpaired electrons in the inner d and f orbitals. Hence, for one electron redox reactions, it is frequently the case that the metal complex will be reduced to a diamagnetic state, i.e., Cu (II)

is reduced to Cu (I), and only the steady-state concentration for the oxidized form of the metal can be detected by ESR.

There are relatively few metal complexes which have been examined in cells and tissues for their redox and radical generating properties. Whatever the reasons for this, it is not for lack of expectation that a variety of reactions will occur. Thus, for example, the area of cellular oxygen chemistry is an important domain of metallobiochemistry. Many of the proteins which interact with oxygen are metalloproteins, including, hemoglobin, cytochrome oxidase, and cytochrome P-450. There is also abundant evidence that the generation of adventitious reduced species of oxygen is a common and deleterious occurrence during oxygen metabolism in an aerobic organism. While these may be initially formed as byproducts of oxygen-dependent enzymatic reaction, further reactions are likely to involve metallo-redox chemistry as described in equations (1)–(3).

$$M_a^n + O_2 \rightleftharpoons M_a^{n+1} + O_2^- \qquad (1)$$

$$M_b^m + O_2^- \rightleftharpoons M_b^{m-1} + O_2 \qquad (2)$$

$$M_b^m + H_2O_2 \rightleftharpoons M_b^{m+1} + OH^- + OH\cdot \qquad (3)$$

Reaction (3) is often referred to as the Fenton reaction in which production of $OH\cdot$ occurs at a faster rate than for the direct reaction of O_2^- with H_2O_2, the Haber-Weiss reaction:

$$O_2^- + H_2O_2 \rightarrow O_2 + OH^- + OH\cdot \qquad (4)$$
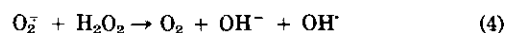
*National Biomedical FSR Center, Department of Radiology, Medical College of Wisconsin, 8701 Watertown Plank Road, Milwaukee, WI 53226.
†Department of Chemistry, University of Wisconsin-Milwaukee, Milwaukee, WI 53201.
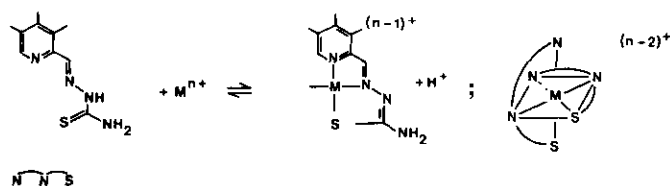‡Author to whom correspondence and reprint requests should be sent.

FIGURE 1. Metal chelation by α-N-heterocyclic carboxaldehyde thiosemicarbazone ligand (also referred to as 2-formylpyridine monothiosemicarbazone) to produce 1:1 and 2:1 ligand-to-metal complexes.

Just as reactive forms of oxygen may be generated by metal-based reactions, so too such entities as superoxide ion and hydrogen peroxide are handled by the metalloproteins superoxide dismutase and catalase which require Fe, Cu(Zn), or Mn. Thus, from many perspectives one expects a wealth of oxygen based radical chemistry to occur when exogeneous complexes of redox metals enter cells.

Copper Complexes as Antitumor and Cytotoxic Agents

ESR Studies of Tridentate Cupric Complexes

More than 20 years ago French and co-workers began synthesizing metal binding ligands as potential antitumor agents with the rationale that they might extract transition metal ions from key sites in cancer cells to inactivate them (4). One class of these ligands is the α-N-heterocyclic carboxaldehyde thiosemicarbazones (Fig. 1), some of which are active as antitumor agents in animals but are not effective in humans (5). Studies on the Cu and Fe complexes of some of the active ligands show that the metal complexes are much more cytotoxic than the parent compounds (6).

Detailed examination of the reaction of 2-formylpyridine thiosemicarbazonato Cu(II) with cell types has led to a scheme for intracellular reaction of the complex (Fig. 2). Upon its addition to plasma or culture media, adduct formation between CuL$^+$ and Lewis bases is observed in the ESR spectrum at 77°K (7). The complex or some adduct species is readily taken up by Ehrlich cells (7). Once in cells, there is little efflux of CuL$^+$, presumably because it is bound to or reacts irreversibly with cellular structures. That cellular adducts of the copper complex do form is shown by the change in its ESR parameters as it enters cells (Fig. 3). The new spectrum taken at 77°K could be modeled by the addition of CuL to excess glutathione, CuL-SG, or to cathemoglobin which has several pairs of reactive thiols, Cu-L-S-CatHb (Fig. 4) (8,9). In the absence of model studies, a good indication of the number of nitrogen, oxygen, and sulfur donor atoms bound to Cu comes from the value of $g_\parallel$ and $A_\parallel$ indicated in Figures 3 and 4, which can be compared to known values with the aid of Peisach-Blumberg plots (10) and from the hyperfine

structure on the high field lines ($g_\perp$ region). The cellular adduct has ESR parameters consistent with an N_2S_2 coordination environment, suggesting as do the model studies that CuL forms adducts with cellular thiols.

Room temperature ESR studies of the interaction of CuL with cells show that the complex displays an immobilized spectrum indicative of its slow motion in solution (Figs. 5 and 6) (11). The intensity of the signal also decreases with time, suggesting that the complex is gradually reduced in cells. For an adduct formed from CuL$^+$ and GSH, the room temperature spectrum should be the isotropically averaged spectrum due to rapid motion of a low molecular weight complex in a medium which is presumably about as viscous as water. Thus CuL most likely forms an adduct with a cysteine amino acid residue from a protein, for the motion for the complex is much slower.

The time course of reaction of other tridentate copper complexes, which are cytotoxic to Ehrlich cells, is similar to that of CuL. Thus, the order of rate of disappearance of the ESR of three such complexes is pyridine-2-carboxaldehyde-2'-pyridylhydrazonate copper (II) > salicylaldehydebenzoylhydrazonato copper (II) ≈ 2-CuL. The net rate of reduction of CuL in cells as measured by ESR is faster than previously observed by following loss of the visible absorbance of the complex (11). However, both in cells and in model studies of the reaction of CuL with glutathione, there is a large increase in oxygen consumption during the total course of reaction. In addition, the thiol content of the systems decreases (7). In the model, there is a burst of production of O_2^- and OH· as measured by spin trapping reactions (7). During the reaction of CuL with GSH, a steady state is reached in which Cu(II)L concentration remains approximately constant, as the complex catalyzes the reaction of oxygen by the sulfhydryl groups of GSH. According to these results, when CuL is taken up by Ehrlich cells a redox cycle is established (Fig. 2) until oxygen is depleted or net reduction of copper is stabilized through the binding of Cu(I) to other sites in the cell. The fact that the room temperature ESR study points to the binding of CuL and the other complexes to protein thiols suggests that this redox cycle may involve the oxidation of important cysteinyl residues of enzymes.

ESR Investigations of Tetradentate Cupric Complexes

The bis(thiosemicarbazone) of 3-ethoxy-2-oxobutyraldehyde and its copper complex, Cu(II)KTS, have excellent antitumor properties in a variety of animal models. In frozen solution the ESR spectrum of CuKTS has a hyperfine structure attributable to the binding of Cu to two equivalent nitrogen donor atoms (Fig. 7). When the complex diffuses into cells this signal disappears rapidly with a pseudo first-order rate constant of 8×10^{-3} sec^{-1} (12). The loss in ESR intensity is consistent with the schematic for CuL (Fig. 2) except adducts with either glutathione or another thiol are not
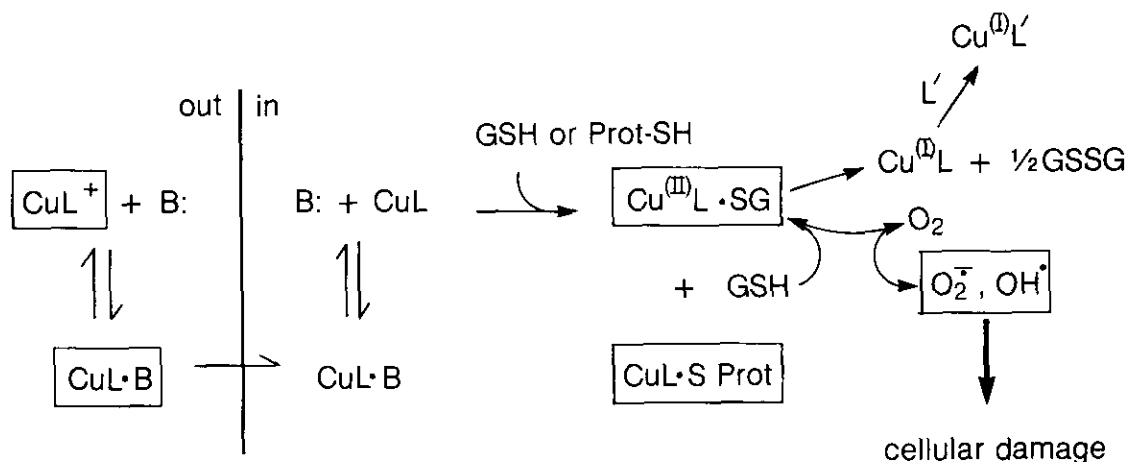
FIGURE 2. Scheme for interaction of CuL^+ with cells. ESR detectable species are enclosed in boxes.

observed. Furthermore, reduction of CuKTS to form Cu(I)SR species occurs in preference to the reoxidation of Cu(I)KTS to Cu(II)KTS by O_2. Thus, there is rapid, reductive dissociation of Cu(II)KTS (12,13). The resultant Cu(I) species are reactive with oxygen to set in motion a redox cycle of Cu(I) and Cu(II), which catalyzes the reduction of oxygen by thiols (12). When Ehrlich cells are titrated with CuKTS, the first major site of binding of Cu(I) is metallothionein, normally a Zn–protein (13). Cu(I)–metallothionein is not rapidly reactive with oxygen (14), so this structure is not involved in the catalysis of oxygen reduction.

The structure of CuKTS has been studied by means of ESR because of its established antitumor properties (13,15–18). The best-resolved ESR spectrum was obtained from CuKTS doped into the nickel analog, NiKTS (18). The principal values of the ESR parameters were used to determine that the copper–ligand bonds are highly covalent and the Cu–N and Cu–S bonds may be regarded as essentially independent.

The function of the bis(thiosemicarbazone) ligand of CuKTS is both to provide a stable form of Cu(II) which can reach tumor cells and to set an appropriate redox potential for the copper center for its reaction in the reductive environment of the cell (12). Thus, 3-ethoxy-2-oxobutyraldehyde-bis(N^4-dimethyl-thiosemicarbazonato) Cu(II), $CuKTSM_2$, has a redox potential about 100 mV more negative than CuKTS (Table 1), reacts very slowly with Ehrlich cells, and at similar concentrations is not cytotoxic to tumor cells (19).

A recent reinvestigation of $CuKTSM_2$ demonstrated that the complex destroys Ehrlich cells at higher concentrations of drug than previously used (13). The complex was known to localize in lipophilic parts of cells, presumably membrane (18). Room temperature ESR studies were undertaken to study $CuKTSM_2$ bound in Ehrlich cells (13). The ESR signal was found to be stable and essentially immobilized in cells (Figs. 8 and 9). As the concentration of $CuKTSM_2$ is increased, a second mobile phase was observed. Coincidently with the tran-

sition from immobilized to mobile $CuKTSM_2$, the cytotoxicity of the complex greatly increases. These ESR results and those with the tridentate copper complexes show clearly the importance of doing ambient temperature ESR measurements to probe the dynamic environment of the complexes.

Bidentate Copper Complexes of 1,10-Phenanthroline and Cytotoxic Agents

It has been known for years that 1,10-phenanthroline inhibits cell proliferation (20). The proposed mechanism has been that this compound acts as a ligand for cellular zinc to mimic a condition of nutrient zinc deficiency, which is also known to inhibit growth (21). Another explanation suggests that a cuprous phenanthroline complex is the active form of the ligand (Fig. 10) (22,23). Indeed, several recent studies have inquired into the reaction of copper–phenanthroline, oxygen, a reducing agent, and DNA to degrade double-stranded DNA into acid-soluble fragments (24–26). As with other copper complexes discussed above, the phenanthroline–Cu complex cycles between Cu(II) and Cu(I) to catalyze the reduction of oxygen to reactive radical species by the reducing agent. Unpublished studies of the reaction of 1,10-phenanthroline with Ehrlich cells lends support to the possible formation of copper–phenanthroline complexes in cells. When the ligand is added to cells, copper redistribution occurs in which Cu(I) metallothionein is found (20). A reasonable intermediate in this reaction would be Cu(I)–1,10-phenanthroline. It is noted that this ligand also causes substantial losses in cellular Zn and Fe, so that its effects on copper are not clearly related to cytotoxicity.

The ESR data for copper doped into a dichloro-1,10-phenanthroline zinc host indicate that the cupric ion is in a distorted tetrahedral structure (27). These parameters, particularly $A_z = 123 \times 10^{-4}$ cm^{-1}, are more characteristic of the type I distorted tetrahedral structure than the square planar structure (27). Bonding pa-
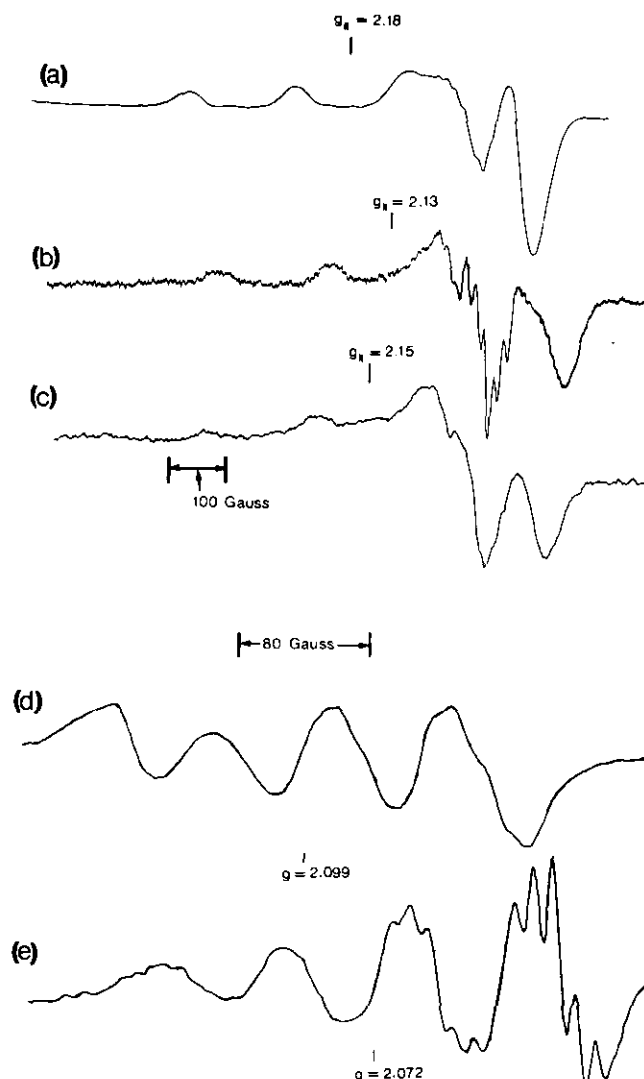
FIGURE 3. Electron paramagnetic resonance spectra of CuL and Ehrlich cells at 77 K. Spectra a, b, and c show EPR spectra of solutions frozen in liquid nitrogen: (a) CuL$^+$ in 0.1 M KCl and 0.25 M sucrose; (b) CuL$^+$ in Ehrlich ascites tumor cells; (c) CuL$^+$ plus excess glutathione. Spectra d, and e show EPR spectra of solutions run in a flat cell at room temperature for CuL$^+$ in KCl at pH 7 in the absence (d) and presence (e) of glutathione. Spectrometer conditions: modulation frequency, 100 kHz; modulation amplitude, 5 G; (a) gain 10×10^2, time constant 1 sec, scan time 4 min, power 5 mW; (b) gain 5×10^3, time constant 3 sec, scan time 8 min, power 5 mW; (c) gain 10×10^3, time constant 10 sec, scan time 1 hr, power 5 mW; (d) gain 5×10^3, time constant 1 sec, scan time 4 min, power 200 mW; (e) gain 5×10^3, time constant 1 sec, scan time 4 min, power 200 mW. From Saryan et al. (7) with permission.

rameters for ternary complexes of Cu–1,10-phenanthroline and amino acids excluding histidine indicate that these adducts have a considerable amount of covalent bonding (28). Nitrogen hyperfine structure appears in the $g_\perp$ region for most of these compounds. More recent infrared and visible studies suggest that ternary complexes with a pyramidal square planar configuration are formed between 1,10-phenanthroline and
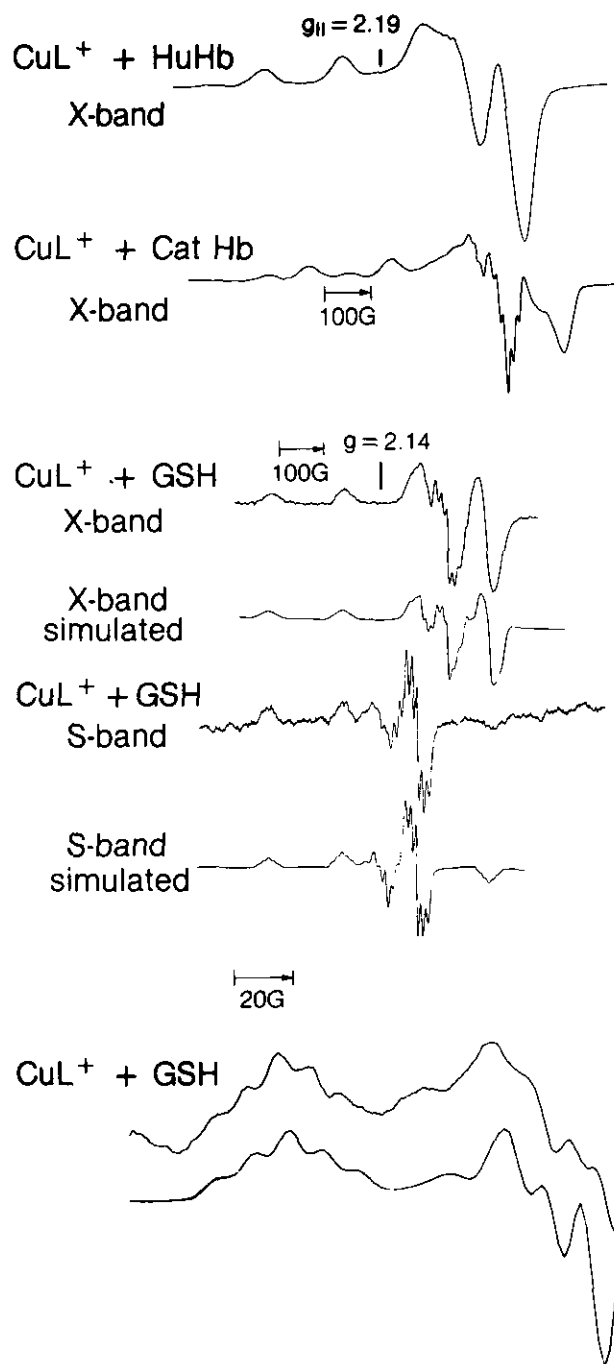

FIGURE 4. X-band EPR spectra for (a) 0.2 mM CuL$^+$ in 5% DMSO plus 0.1 mM human Hb and (b) 2 mM CuL$^+$ plus 2 mM cat Hb in 0.1 M NaCl and 0.15 M phosphate buffer at pH 7.4. Spectrometer conditions: incident power 5 mW, mod 5 G, at $-196°C$. (c–f) Experimental and simulated spectra for ^{65}CuL$^+$ (1.3 mM) in 0.05 M bis Tris buffer plus mM glutathione and a final pH of 6.9. X-band spectrum; X-band simulated spectrum; microwave frequency 9.129 GHz, $g_\parallel$, $g_\perp$ = 2.035, $A_\parallel$ = 180×10^{-4} cm^{-1}, $A_\perp$ = 30×10^{-4} cm^{+1}, A_N = 12×10^{-4} cm^{+1}, parallel linewidth 8.0 gauss, perpendicular linewidth 6.0 gauss; S-band spectrum; S-band simulated spectrum: microwave frequency 3.32 GHz. (g,h) Expansion of m_I = -1/2 line in $g_\parallel$ region and $g_\perp$ region for X-band experimental and simulated spectra. Conditions as in Figure 2. From Antholine and Taketa (8,9).
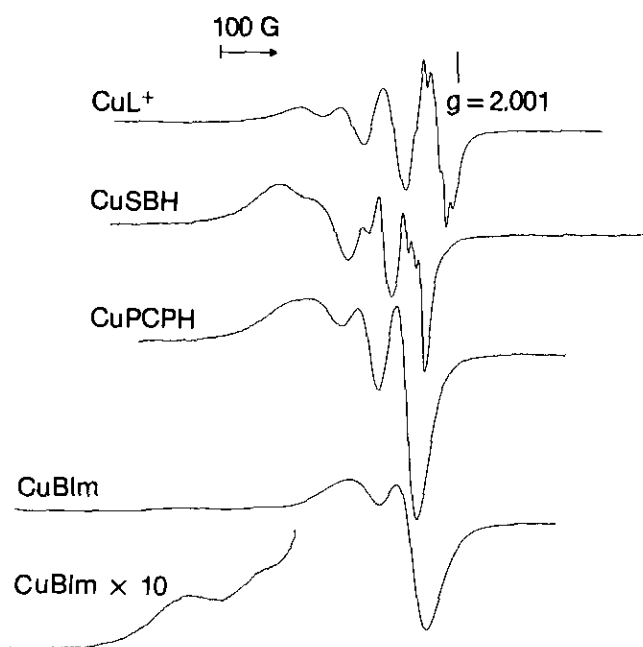
FIGURE 5. X-band ESR spectra at room temperature for CuL$^+$, CuSBH, CuPCPH in DMSO, and CuBlm in 0.1 M NaCl at pH 7. Spectrometer conditions: incident microwave power 200 mW, microwave frequency 9.504 GHz, modulation amplitude 5 G, modulation frequency 100 kHz, ESR flat cell used for samples. (CuL$^+$) 2-Formylpyridine monothiosemicarbazonato copper (II); (CuSBH) salicylaldehydebenzoylhydrazonato copper II; (CuPCPH) pyridine-2-carboxaldehyde-2'-pyridylhydrazonato copper (II); (CuBlm) cupric bleomycin. From Antholine et al. (11).

copper–dipeptide complexes (29). ESR parameters from room temperature and frozen solutions were tabulated but no nitrogen hyperfine splittings were resolved. It is suggested that the peptide supplies three donor atoms to the square plane and one nitrogen from 1,10-phenanthroline occupies the fourth planar position, while the other atom occupies the apical position. This
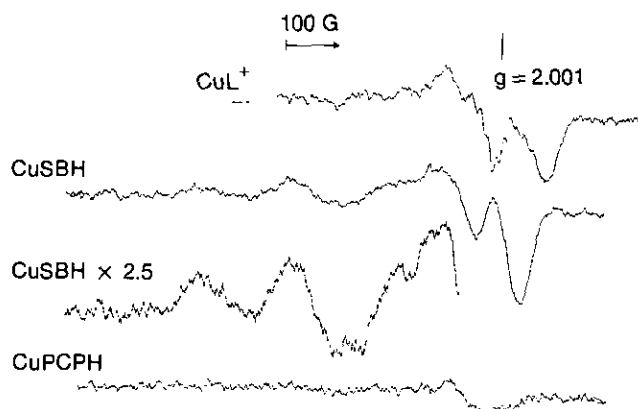

FIGURE 6. X-band ESR spectra at room temperature of CuL$^+$ (initial conc. 6 mM), CuSBH (initial conc. 7 mM), and CuPCPH (initial conc. 8 mM) in 10^8 Ehrlich cells suspended in 0.15 M NaCl. See Fig. 5 for names of copper complexes. From Antholine et al. (11).
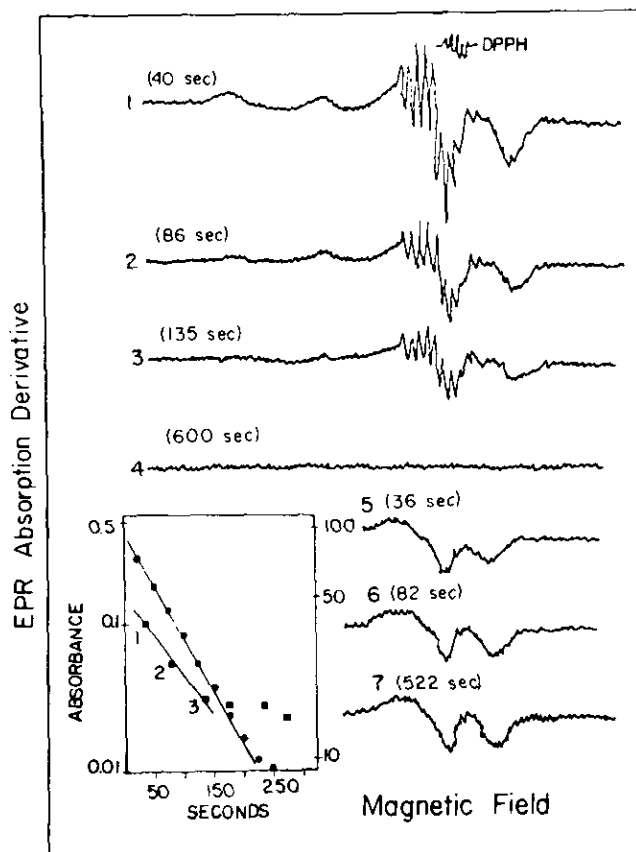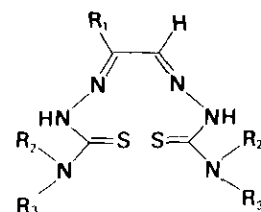

FIGURE 7. Structure for H$_2$ KTS for which R = is ethoxyethyl and R$_2$, R$_3$ = H; electron paramagnetic resonance spectra of reaction of copper complexes with cells: (1–4) time dependence of spectra of CuKTS; (5–7) time dependence of spectra of CuCl$_2$. Inset: first-order kinetic plot of (■) the loss of EPR intensity and of (●) absorbance of the same sample of CuKTS and cells. Cell suspension, 27.5 mg/mL; 4.5 × 10^7 cells/mL; [CuKTS]$_{initial}$, 1.55 × 10^{-4} M. From Minkel and Petering (12).

adduct is, in a sense, the mirror image of the adduct of CuL and protein. CuL is a tight tridentate complex, and the protein supplies the fourth donor atom to complete the square planar configuration or a fourth donor atom and an atom which binds in an axial position to complete the square pyrimidal configuration. Nitrogen atoms from 1,10-phenanthroline (L') complete the square pyramidal configuration while the protein provides the tight tridentate binding site.
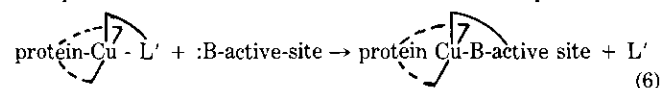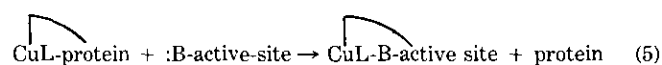
Although additional information about the speciation of coordinately unsaturated copper complexes in cells needs to be obtained, one can imagine subtle differences

Table 1. Redox properties of copper and iron complexes of some known antitumor agents.

| Complex | Ligand | Structure[a] | | | | $E_{1/2}(CuL^+)$, mV | $E_{1/2}(FeL_2^+)$, mV | Reference |
		R_1	R_2	R_3	R_4			
	HL-CF$_3$					124	386	(94)
	HL-Cl					37	311	
	HL-H					2	242	
	HL-CH$_3$					19	209	
	HL-OH					− 29	24	
	HL-N(CH$_3$)$_2$					− 51	52	
	H$_2$KTS					−178		(95)
	H$_2$KTSM					−188		
	H$_2$KTSM$_2$					−283		
CuKTS		CH(OEt)CH$_3$	H	H	H			
CuKTSM				CH$_3$	H			
CuKTSM$_2$				CH$_3$	CH$_3$			

[a] Key for structures:

ML-X
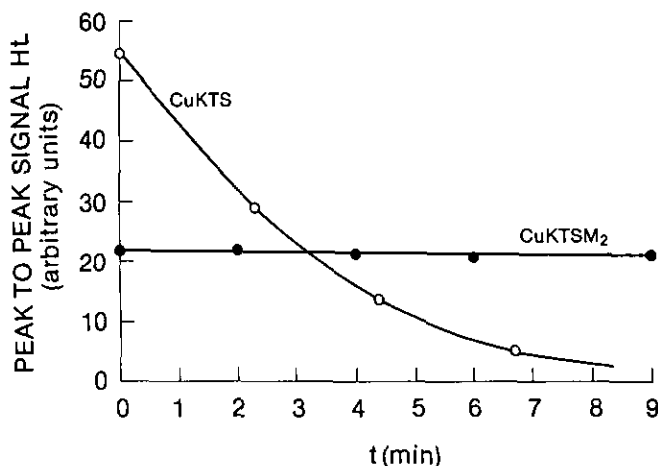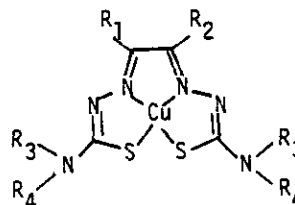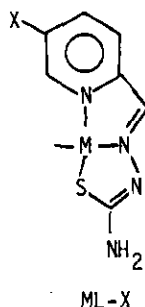
FIGURE 8. Disappearance of CuKTS (0.6 mM) ESR signal at room temperature but not CuKTSM$_2$ (0.6 mM) after addition to 6 × 10^7 Ehrlich ascites tumor cells/mL of cell suspension. From Antholine et al. (13).

in their mechanisms of reaction may exist [Eqs. (5) and (6)].

$$CuL\text{-protein} + :B\text{-active-site} \rightarrow CuL\text{-B-active site} + protein \quad (5)$$

$$protein\text{-}Cu \text{ - } L' + :B\text{-active-site} \rightarrow protein\ Cu\text{-B-active site} + L' \quad (6)$$

Thus the upper reaction would transfer the antitumor

agent to the active site containing a Lewis base site (B:) and release the protein carrier, while the lower reaction would crosslink proteins and other macromolecules and release the original copper-binding ligand, L'. ESR data of the oxidized forms of copper introduced into cells may be used to identify its speciation to substantiate or refute hypothetical reactions such as those suggested above.

Another class of copper complexes with cytotoxic activity has been discovered in the investigation of the report that cells treated with diethyldithiocarbamate (dtc) are more susceptible to bleomycin (Blm), a drug discussed in following sections, than control cells (30). The dtc was thought to enhance the effect of Blm either by inhibiting superoxide dismutase which results in an increase of O_2^- and/or by reducing the level of weakly bound and kinetically available Cu^{2+} in the cell which could bind and inactivate bleomycin in the strand scission of DNA, the putative mechanism of cytotoxicity of this drug (31). Recent data of Ujjani and Petering indicate that Cu(dtc)$_2$ is substantially more toxic than dtc under metal-free conditions. EPR studies indicate that 0.54 mM Fe(III) Blm is almost completely stable in the presence of about 20 mM dtc for at least 10 min. In contrast, 0.27 mM Cu(II) Blm is rapidly and completely converted to Cu(dtc)$_2$ + Blm upon addition of 0.92 mM dtc. Clusters or aggregates of Cu(dtc)$_2$ are formed consistent with the low solubility of Cu(dtc)$_2$ in aqueous solvents, which probably helps pull the reaction toward Cu(dtc)$_2$. Thus, dtc may enhance the activity of Blm by limiting its reaction with cellular copper. However, to the extent that Cu(dtc)$_2$ forms in cells, a new, highly cytotoxic copper complex is generated which independently augments the effects of Blm.
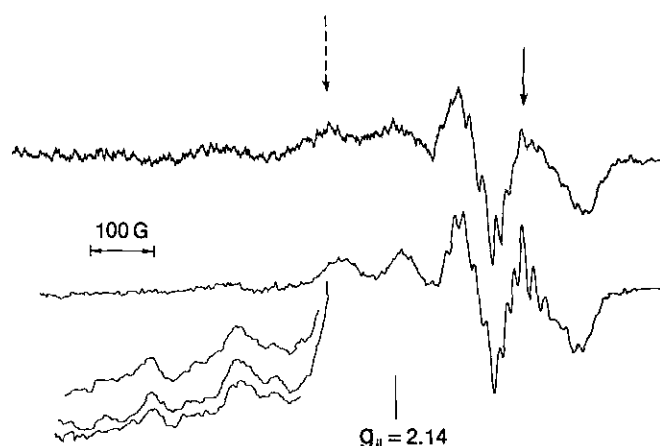
The ESR spectrum of Cu(dtc)$_2$ has been well studied (*32–34*). The use of dtc to measure quantitatively inorganic cupric ions using ESR has been reviewed by Janzen (*35*). The source of a copper ESR signal previously observed in fatty tissues has been identified as Cu(dtc)$_2$. This complex is formed through contact of copper-containing tissue with surgeon's gloves laced with dtc-like complexes (*36*). Cu(dtc)$_2$ levels of 0.5 μM can be detected in tissues because the ESR lines are very sharp for this copper complex. Besides sensitivity, Cu(dtc)$_2$ complexes are expected to form adducts in complex biological systems. Model ESR studies have already shown that mixed complexes of the type Cu(dtc)X can be identified (*37*).

$$Cu(dtc)_2 + CuX_2 \rightleftarrows 2\,Cu(dtc)X \qquad (7)$$
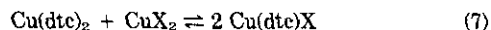
In summary, paramagnetic copper complexes and their adducts should form in cells and be relatively stable in cells depleted of reducing equivalents. Detection and isolation of these adducts in cells is, in our opinion, the next step to better understanding for the interaction of cupric forms of these antitumor agents with cells.

ESR Studies of Cupric Bleomycin

Bleomycin is a clinically used antitumor agent (Fig. 11). It is isolated from *Streptomyces verticillus* as a copper complex (*38*). Although CuBlm is an active antineoplastic drug, it is inactive in the cleavage of DNA, a reaction thought to be the molecular basis of cytotoxicity (see FeBlm, below) (*31,39,40*). An inquiry into the redox reactivity of CuBlm with thiols such as glutathione and oxygen demonstrated that in contrast to the tridentate thiosemicarbazonato copper complexes, there is little redox cycling of copper and little reduction of oxygen as reductive dissociation occurs (*31,41–43*).

ESR studies generally have supported the contention that the cupric site in CuBlm is square pyramidal (*44–50*). Data from electron spin echo spectroscopy, which is useful for determining whether imidazole is a ligand, confirms that an imidazole is involved in the binding of cupric ion (*51*). Nitrogen hyperfine structure is better resolved in both the $g_\parallel$ and $g_\perp$ regions at lower microwave frequencies (S-band) than at the commercial frequency (X-band) (*52*). Computer simulation of the S-band spectra suggests that cupric ion binds to four donor nitrogen atoms, three with $A_N = 10$ G and one with $A_N = 15$ G. ENDOR data confirm the assignment of at least two inequivalent nitrogens with couplings of 11 and 15 G (*52*). In addition, six proton couplings are well resolved in the ENDOR spectra, and the matrix ENDOR indicates that H$_2$O is accessible to the metal site.

Ambient temperature ESR studies of CuBlm have also been carried out at several microwave frequencies to obtain rigid limit parameters for the complex in the liquid phase (*53*). We have argued that the cupric bleomycin structure opens up at room temperature and that the cupric ion is displaced from the square plane (*53*). Not only is the work important from the standpoint of the reactivity of an important antitumor complex, but these studies are fundamentally important as model studies. Thus, the comparison of complexes in frozen and mobile states can reveal dynamic changes which occur upon changing from the immobile, frozen state to the mobile, fast tumbling, liquid state. For example, analysis of the rotational correlation time suggests that copper bleomycin is cigar shaped or has segmented flexibility and rotates about a hinge (*53*).

It occurred to us that Zn^{2+} and especially Cd^{2+} might also form five-coordinate square pyramidal structures with Blm. If Cd^{2+} binding to Blm was analogous to Cu^{2+}, the structure of the ligand, Blm, could be determined from C-13 NMR in the presence of diamagnetic Cd^{2+}. C-13 NMR spectra in the presence of Cu^{2+} are so broadened and shifted that useful structural data has not been forthcoming. Unpublished cadmium-113 NMR results at temperatures lower than ambient temperature suggest that the secondary amine, for which lines are broadened and shifted, as well as the primary amine, the pyrimidine nitrogen, and the imidazole nitrogen are bound to Cd. The latter three donor atoms are directly implicated from the examination of ^{113}Cd-Blm in which two-bond and three-bond ^{113}Cd–^{13}C spin-spin couplings are observed at carbons associated with these potential ligand sites (*54*). As the temperature approaches ambient temperature only the primary amine, the pyrimidine nitrogen and the imidazole nitrogen from Blm are
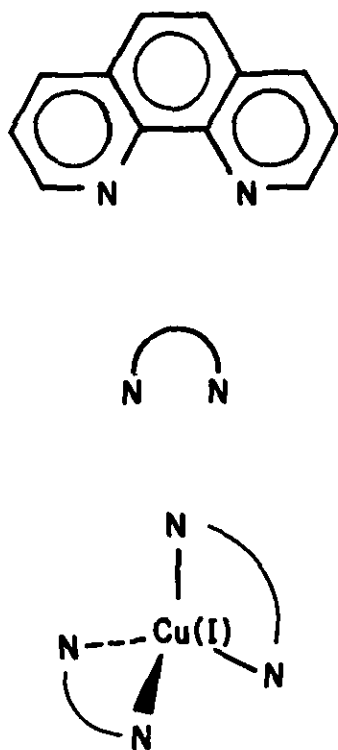
FIGURE 10.   Schematic for cuprous phenanthroline complex.

bound to Cd-113. The Cd-113 isotope was also used to monitor the Cd-113 NMR spectrum of the metal itself. These data indicate that a solvent anion is bound, for example chloride ion, at ambient temperature but not at lower temperatures. Both the NMR data for CdBlm and the ESR data for CuBlm at ambient temperature substantiate a change in structure as a function of temperature. We intend to use these techniques to probe how metal complexes of Blm react in media such as tumor cells, which may involve mechanisms not easily envisioned from data in the static state.

Finally, no evidence exists from low temperature ESR studies to support the formation of CuBlm–Lewis base ternary complexes such as CuBlm–pyridine adducts. However, at room temperature our first indication of ternary complex formation comes from the ESR data for CuBlm in the presence of a large excess of pyridine (11). Pyridine slows down the motion of CuBlm presumably because a ternary complex is formed; the shape of the complex also becomes spherical. Preliminary studies do suggest that CuBlm forms adducts in the presence of cells similar to the pyridine adduct (11).
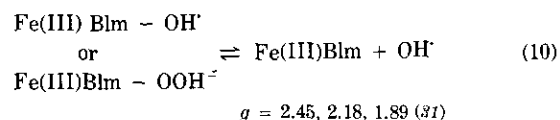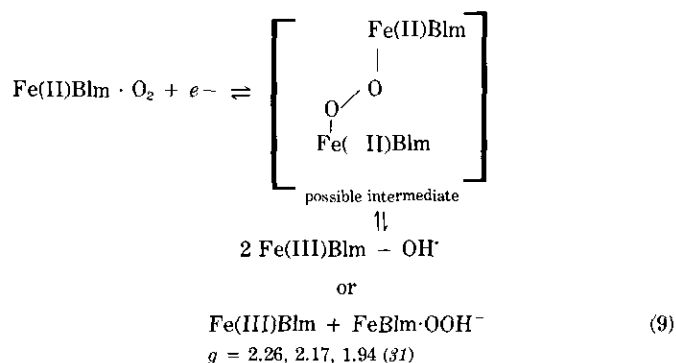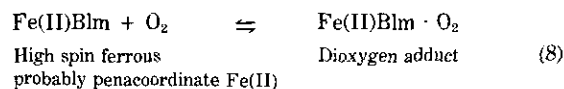
Iron Complexes as Antitumor and Cytotoxic Drugs

ESR Studies of Iron Bleomycin and Co(II) Blm and Ni(III) Blm

Interest in the properties of iron bleomycin (FeBlm) was enormously increased in 1978 by reports of Hor-

witz, Peisach and co-workers that Fe^{2+} greatly stimulates the oxygen-dependent DNA strand scission activity of Blm (40,41). Since the degradation of DNA by this drug had been thought to cause cytotoxicity, it was suggested that Fe(II)Blm may be the biologically active form of the glycopeptide.

A number of elegant studies by Peisach's group (32,56–58), together with results of Sugiura (59–66) have led to the current view of oxygen activation by Fe(II)Blm shown in Eqs. (8)–(10).

$$Fe(II)Blm + O_2 \rightleftharpoons Fe(II)Blm \cdot O_2$$

High spin ferrous   Dioxygen adduct   (8)
probably penacoordinate Fe(II)

$$Fe(II)Blm \cdot O_2 + e^- \rightleftharpoons \begin{bmatrix} Fe(II)Blm \\ | \\ O \diagup O \\ | \\ Fe(II)Blm \end{bmatrix}$$

possible intermediate

$$2 Fe(III)Blm - OH^-$$

or

$$Fe(III)Blm + FeBlm \cdot OOH^- \qquad (9)$$

$$g = 2.26, 2.17, 1.94 \; (31)$$

$$\begin{array}{l} Fe(III) \; Blm - OH^- \\ \qquad \text{or} \qquad \rightleftharpoons Fe(III)Blm + OH^- \quad (10) \\ Fe(III)Blm - OOH^- \end{array}$$

$$g = 2.45, 2.18, 1.89 \; (31)$$

The intermediate, Fe(III)Blm–OH· or Fe(III)Blm–OOH⁻, was shown to be an iron-oxygen adduct with the use of $^{17}O_2$ ($I = 5/2$) (31). This trapped intermediate has broadened ESR lines. The ESR spectrum arises from Fe(III) and not a free radical and Fe(IV) because with ^{57}Fe, $I = 1/2$, the $g = 1.94$ line is clearly split into a doublet indicating hyperfine interaction from the nuclear spin of iron.

The electronic nature of this intermediate is of interest. Its g values are contracted toward the free-electron value relative to Fe(III)Blm, presumably because of the quenching of orbital angular momentum. The g values of Fe(III)Blm are similar to those of iron prophyrins, suggesting the presence of four in-plane nigrogen donor atoms. In the iron–porphyrin system, g-value contraction only occurs when axial sulfur donor atoms replace oxygens or nitrogens (65). A similar effect is seen in Fe(III)Blm adducts (58,66). The only sulfur atom in Blm is part of the bithiazole moiety and is not thought to bind to iron in the intermediate. However, in a recent NMR study it was shown that the bithiazole group of excess Blm interacts with iron in Fe(II)Blm and NO–FeBlm, so it is plausible that bithiazole sulfur may act
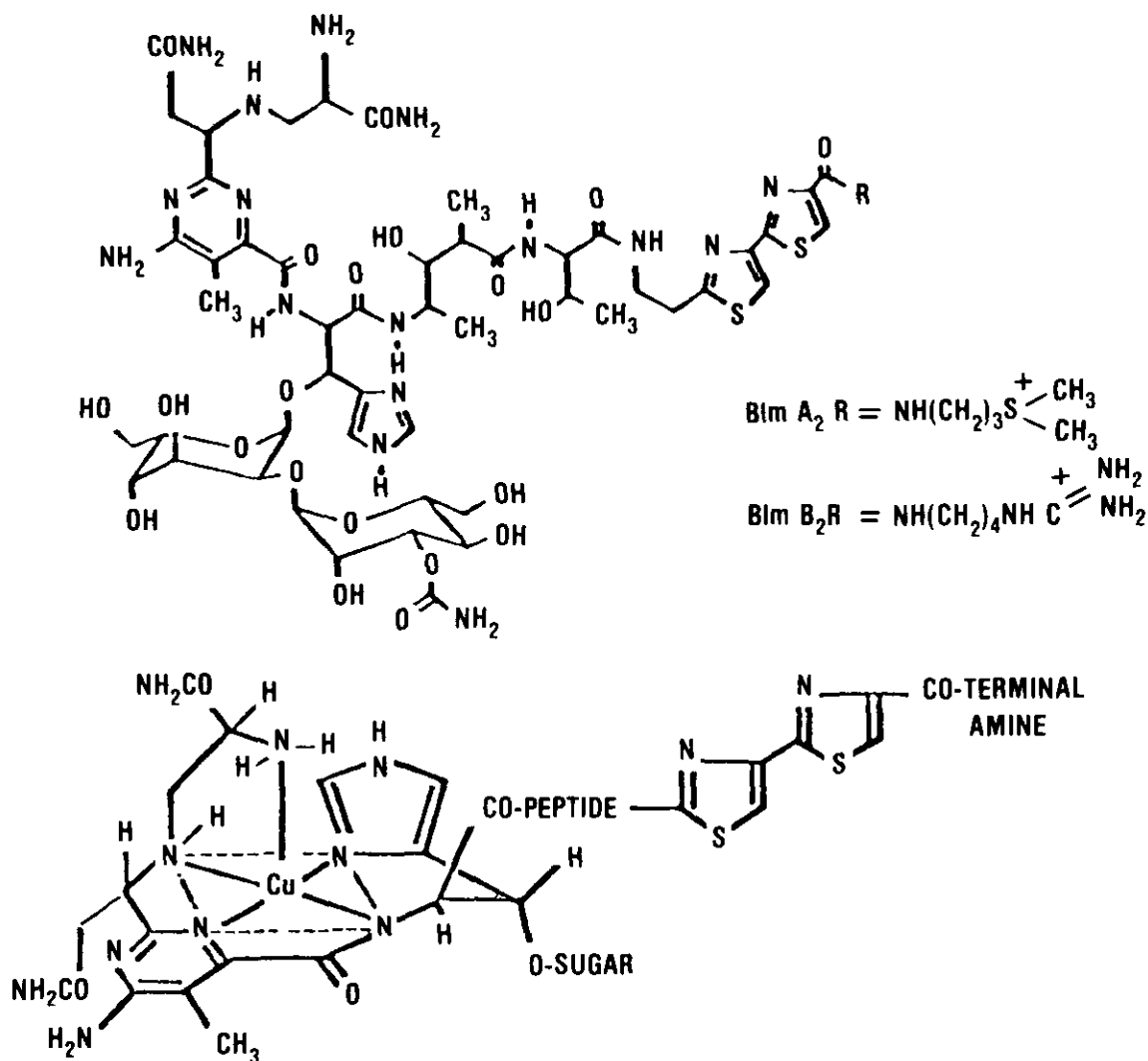
FIGURE 11. Structures for bleomycin (Blm) and CuBlm.

as a ligand in some intra- and intermolecular complexes of FeBlm (67).

Spin-trapping studies have demonstrated that the redox process summarized in reactions (1)–(3) generates a large flux of hydroxyl radicals (41,63,64,68). Although OH· was thought to initiate strand scission, the addition of scavengers for OH· or for O_2^-, and H_2O_2 to the reaction mixture does not affect the yield of degraded DNA (69). Thus free reduced-oxygen species are not involved in attack on the backbone of DNA. In fact, since kinetics of conversion of the product of reaction (9) to Fe(III)Blm and the rate and extent of DNA strand cleavage are identical, it is suggested that a bound form of oxygen, Fe(III)Blm-OH· or Fe(III)Blm-OOH⁻, insensitive to radical scavengers, is the reactive species (31). This conclusion was beautifully supported by the demonstration that in the presence of H_2O_2, Fe(III)Blm was converted to the same intermediate as formed when Fe(III)Blm reacts with O_2^-.

$$2 \text{ Fe(III)Blm} + H_2O_2 \rightleftharpoons 2 \text{ Fe(III)Blm—OH·}$$

or

$$\text{Fe(III)Blm} + \text{Fe(III)Blm—OOH} + H^+ \qquad (11)$$
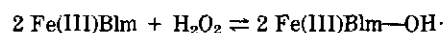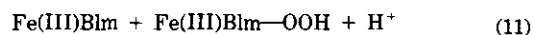
and that this intermediate degrades DNA (31).

The reductant to cleavage site stoichiometry for the DNA strand scission reaction is thought to be 4–5 to 1. Thus, at least two electron equivalents are required beyond those generated in reactions (8) and (9). Indeed, it is unlikely that the principal source of reducing equivalents in cells is Fe^{2+} because of its very small free concentration. An alternative is that the other cellular reductants such as thiols may supply electrons for the overall reaction. In one study the authors demonstrated that cysteine but not glutathione stimulates the reaction of Fe(III)Blm with DNA (67). However, GSH enhances the amount of strand scission caused by Fe^{2+} and Blm, which suggests that thiols can supply electrons
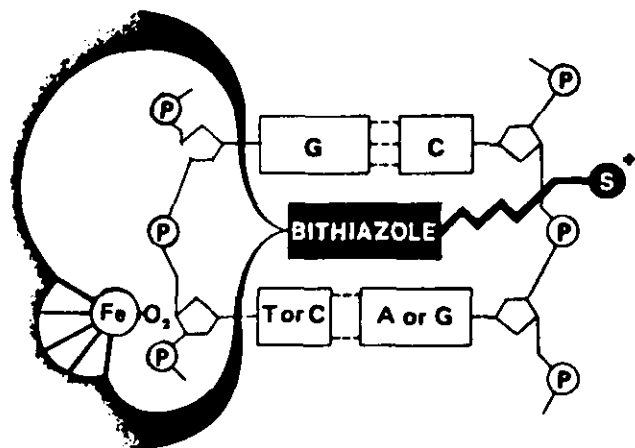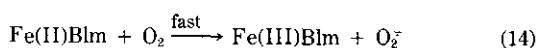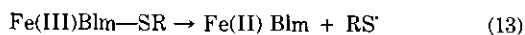
FIGURE 12. Model for the complex of bleomycin, DNA, Fe^{2+}, and O_2. From Takashita et al. (70) with permission.

to the process beyond the formation of the intermediate in reaction (9). Interestingly, although thiols are often thought to protect against radicals, in the presence of redox-active metal sites and oxygen, they may enhance radical production.

The thiol dependent reduction of Fe(III)Blm has been examined by ESR spectroscopy (66). Under aerobic conditions, a redox cycle is established as shown in Eqs. (12)–(14).

$$Fe(III)Blm + RSH \rightleftharpoons Fe(III)Blm{-\!\!-}SR + H^+ \qquad (12)$$

$$Fe(III)Blm{-\!\!-}SR \rightarrow Fe(II)\ Blm + RS^· \qquad (13)$$

$$Fe(II)Blm + O_2 \xrightarrow{fast} Fe(III)Blm + O_2^- \qquad (14)$$

In the steady state a species with contracted g values (2.32, 2.18, 1.935) similar to those of the product of reaction (9) above forms, which is quite stable in the case of Fe(III)Blm + GSH. This intermediate is taken to be Fe(III)Blm–SR.

Another essential feature of the mechanism of reaction of FeBlm with DNA is that the bithiazole and terminal cationic portion of Blm can intercalate and bind to DNA, thus bringing the reactive iron site into close proximity with the DNA backbone (Fig. 12) (70). Although the metal coordination and DNA binding sites are frequently portrayed as relatively independent of one another, an ESR study of Fe(II)Blm·NO; and its DNA adduct clearly shows that the electronic spectrum of the Fe-NO species is perturbed upon binding of the complex to DNA (Fig. 13) (71,72). Analysis of the perturbation suggests that it is occurring in the x–y plane of the metal coordinate site. Interestingly, NMR studies of the interaction of Fe(II)Blm-CO with poly(dA-dT) also indicate changes in the iron-binding site, particularly in proton resonances from imidazole, which is thought to be an in-plane ligand of Fe (67).

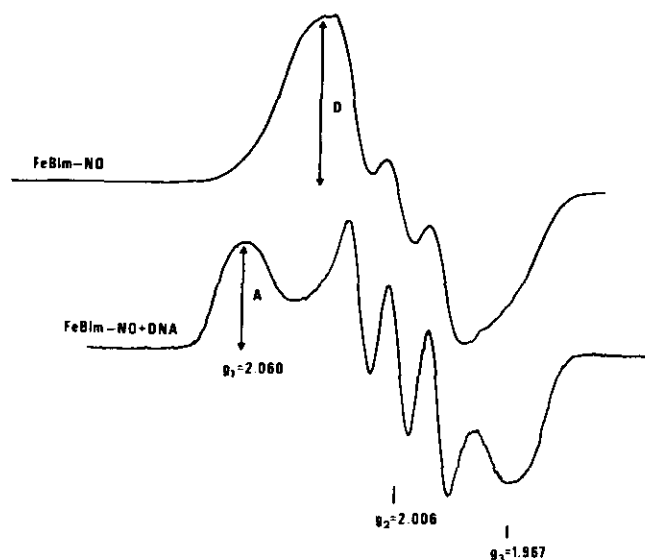Sugiura has examined the ESR properties of the

FIGURE 13. EPR spectrum of a frozen (−196°C) solution of 0.1 mM FeBlm- NO. (a) in the absence and (b) the presence of 18 mg/mL of calf thymus DNA and 0.15 M phosphate buffer at pH 7.2. From Antholine and Petering (71).

Fe(III) complexes of a number of modified bleomycins (58). He concluded that the structure of the iron binding site was five-coordinate, probably similar to the structure of a biosynthetic intermediate of a Cu(II)Blm (Fig. 14). In this structure, the primary amine of Blm acts as an axial base and four nitrogen donors supply the ligands of the xy plane. This would leave the sixth coordinate site open to bind oxygen in the Fe(II) complex. When the adjacent terminal amine is hydrolyzed to yield a carboxyl group, the amine and carboxyl compete for the fifth coordination site in a pH-dependent way (58). At pH 7, the carboxyl is bound and no DNA strand scission occurs. Furthermore, the complex is now high spin with a $g = 4.28$ signal. Thus, like hemoglobin, its spin state changes with the nature of the axial ligand and presumably its oxygen activation properties do, as well.
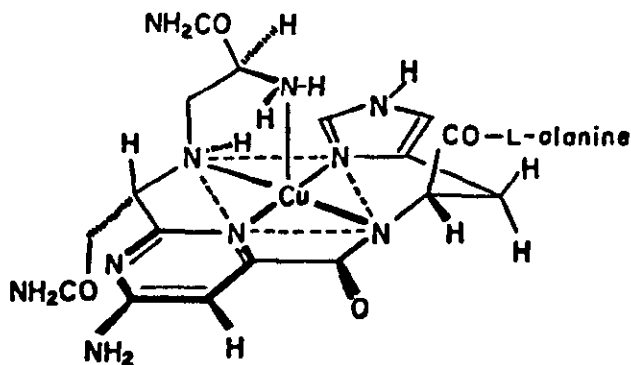

FIGURE 14. Structures of Cu(II)-complex of P-3A. From Iitaka et al. (44) with permission.

Studies of the pH-dependence of the ESR spectrum of Fe(III)Blm show that it undergoes a transition from low to high spin with an apparent pK_a of 6.5 prior to completely dissociating at lower pH (Fig. 15) (71). Possibly, this transition involves the protonation and dissociation of the axial amine group as suggested by Sugiura's studies described above. The spin-state change can also be accomplished by the titration of Fe(II)Blm with phosphate (Fig. 16). A first hypothesis to explain the effect is that phosphate competes with the axial amine much as a carboxylate oxygen does in the depyruvamide Blm complex described above. However, the phosphate adduct is competent to carry out DNA strand cleavage. Fe(II) depyruvamide Blm is not (58).

ESR spectroscopy of Co(II)Blm and Ni(III)Blm has helped to characterize the metal binding site of the glycopeptide. The ESR spectrum ($g_{\parallel} = 2.206$, $g_{\perp} = 2.272$, $A_{\parallel}^{Co} = 92.5$ G, and $A^N = 13$ G) for Co(II)Blm in the presence of DNA and in the absence of oxygen is typical for square pyramidal Co(II) complexes with the unpaired electron in the d_z^2 orbital (73). The three-line nitrogen hyperfine structure on one of the eight lines ($I = 7/2$) in the $g_{\parallel}$ region indicates that the apical part of the ligand is a nitrogen donor atom. We have obtained

an unpublished spectrum of Co(II)Blm in the absence of DNA which is better resolved than the previously published spectra (Fig. 17). This spectrum has an apparent 1-2-3-2-1 pattern consistent with two axial nitrogen donor atoms. The ESR spectrum for Ni(III)Blm also has a five line 1-2-3-2-1 pattern on the $g_{\parallel}$ feature (74,75). This again indicates the presence of two axial nitrogen donor atoms in the absence of DNA. Interestingly, the spectrum of the Ni(III) P-3A fragment has a single nitrogen donor atom consistent with the 1-1-1 three-line hyperfine pattern in the $g_{\parallel}$ region consistent with a single axial nitrogen donor atom (74). Upon addition of oxygen, oxygen is bound in an axial position to Co(II)Blm and alters the ESR parameters ($g_{\parallel} = 2.098$, $g_{\perp} = 2.007$, $A_{\parallel}^{Co} = 20.2$ G, $A_{\perp}^{Co} = 12.4$ G) (75). As with FeBlm·NO, the addition of Co(O$_2$)Blm to DNA changes the ESR parameters ($g_{\parallel} = 2.106$, $g_{\perp} = 2.004$, $A_{\parallel}^{Co} = 18.9$ G, $A_{\perp}^{Co} = 11.5$ G) (75), which argues for an interaction of the metal-binding site with DNA. A pH-dependent change in ESR parameters was attributed to a change in axial ligation from a nitrogen to an oxygen donor atom. The Co(II) complex and its dioxygen adduct of deamino-Blm which lacks the primary amine (purportedly the axial moiety) provide a model
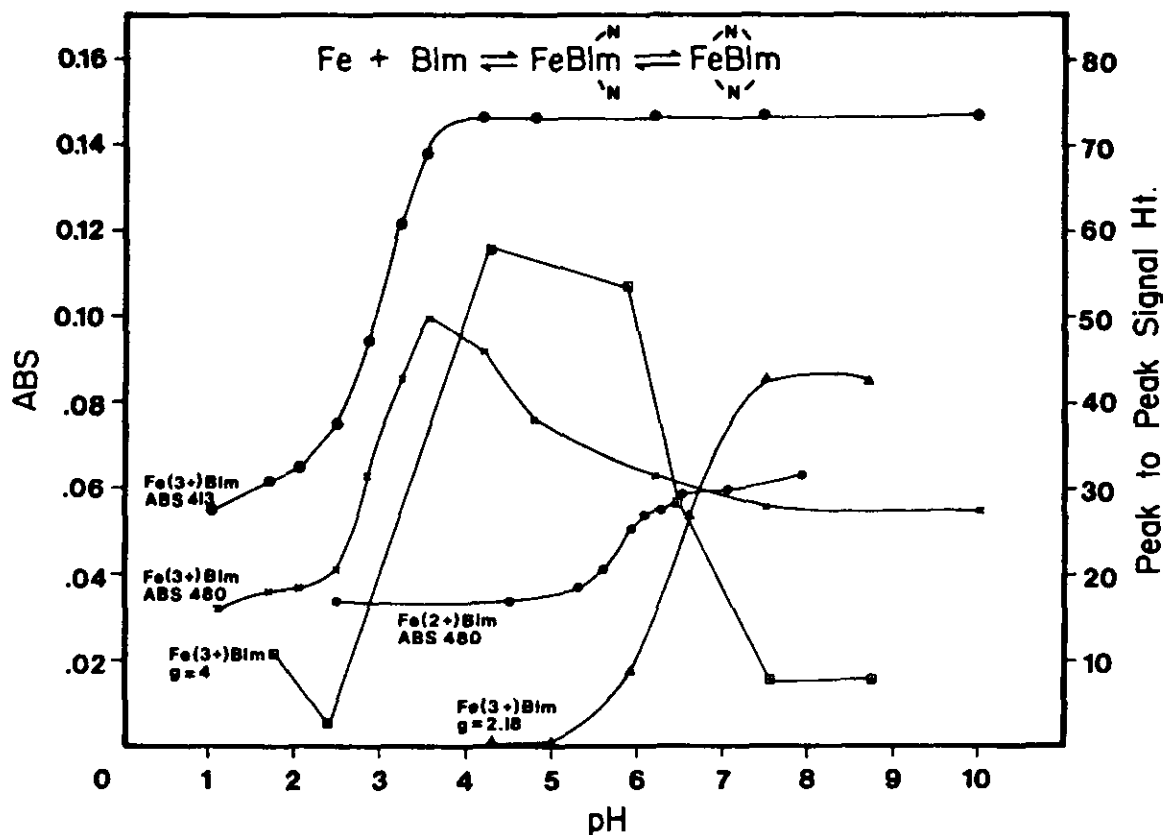
FIGURE 15. pH dependence of the absorbance at 413 nm and 480 nm for Fe^{3+}Blm and at 480 nm for Fe^{2+}Blm (left ordinate) in addition to the pH dependence versus the peak to peak signal height (right ordinate) for high spin Fe^{3+}Blm at $g = 4$ and low spin Fe^{3+}Blm at $g = 2.18$. All solutions are made up in 0.1 M NaCl. The concentration of both Fe^{3+}Blm and Fe^{2+}Blm is approximately 0.2 mM. From Antholine and Petering (71).
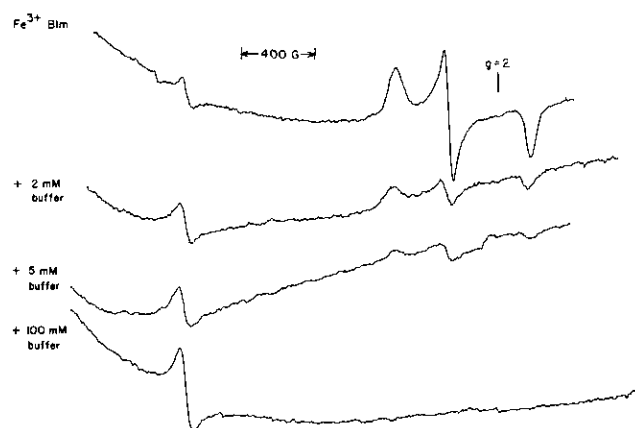
FIGURE 16. ESR spectra for Fe(III)Blm as the concentration of phosphate buffer is increased. The final pH was 7.5. The curvature in the baseline is due to an impurity in the Dewar and varies with the position of the Dewar.

in which the axial donor atom reverts from a nitrogen donor atom to an oxygen atom (73,76). These studies with CoBlm and NiBlm probe two facets of Blm chemistry which are not as clearly described for FeBlm. Namely, Blm itself contains a multitude of potential donor atoms. A single nitrogen axial donor atom can orient the molecule into a square pyramidal configuration or two nitrogen axial donor atoms can change the Blm metal site into a rhombic octahedral configuration. Upon binding to DNA presumably through intercalation of the bithiazole group, the metallobleomycin structure reorients from rhombic to square pyramidal.

ESR Studies of Iron Adriamycin, Fe(Adr)₃

The early suggestion that an iron–adriamycin complex, quelamycin, ameliorates the cardiac toxicity of adriamycin has not been substantiated in other investigations (77,78). One of the problems with this work was the use of a mixture of iron and Adr with a stoichiometry of Fe₃Adr, which does not represent the actual coordination stoichiometry Fe(Adr)₂ or Fe(Adr)₃ (77). Recently, an iron adriamycin complex that has been difficult to characterize has been shown to bind to erythrocyte ghost membranes and is involved in lipid peroxidation (79). Other work indicates that an Fe(II)–adriamycin complex bound to DNA damages DNA, presumably via a hydroxyl radical. A cycle similar to the cycle for CuL discussed previously has been proposed for the redox chemistry of iron adriamycin in cells. A schematic for this cycle taken primarily from the excellent work of Myers and co-workers is as follows (Fig. 18).

The reaction of iron adriamycin with membrane has not been observed with either CuL or FeBlm. On the other hand, the damage to DNA from hydroxyl radical appears to be quite similar to the damage caused by FeBlm.

The only ESR studies to our knowledge of
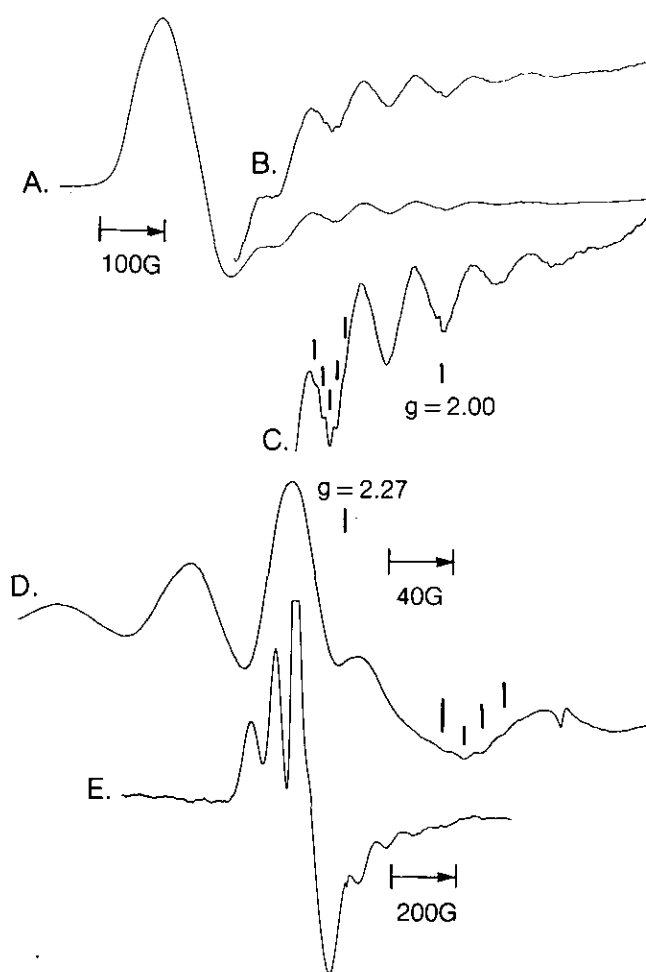
FIGURE 17. X-band (A–C) and S-band (D,E) spectra for 8.6 mM CoBlm. The five hyperfine lines on a cobalt line in the $g_\parallel$ region indicate that two nitrogen donor atoms are in apical positions. The sample was prepared, the pH adjusted to 7.5 (or above) and the sample frozen under a nitrogen atmosphere in a glove box.

$Fe^{3+}(Adm)_3$ show that the ESR signal consists of two lines at $g = 2.01$ and $g = 4.2$ (80). Although the origin of the lines has not been discussed, it is presumed that the lines arise from occupancy of different Kramer's doublets of a high spin iron complex (81). In the absence of oxygen, a new line appears at $g = 2.34$, reaches a
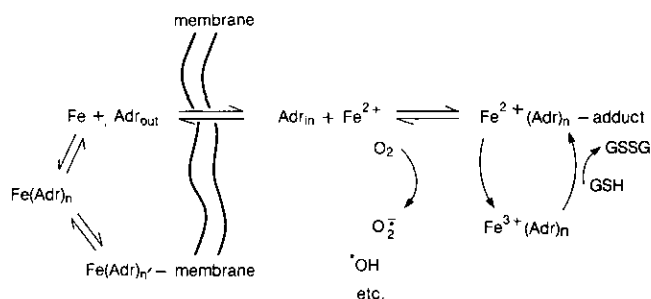
FIGURE 18. Scheme for interaction of iron-Adriamycin with cells.

maximum at about 130 min after complex formation, and disappears (*80*). During this reduction of iron–Adriamycin, a signal at $g = 2.01$ may appear which, except for the g value, appears to be a free-radical signal (*82*). Since the $Fe(Adm)_3$ spectrum returns on exposure to oxygen, it is concluded that $Fe(Adm)_3$ is slowly reduced to a ferrous Adriamycin complex and then reoxidized. Even though some of the details concerning the characterization of the iron and radical signals are not yet published, these signals are consistent with a hypothesis whereby reactive, reduced oxygen and Adriamycin radicals are generated in the presence of iron, which may have significant biological activity as described in the next section (*83–85*).
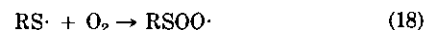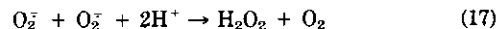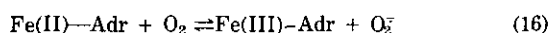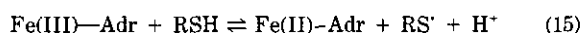
Radical Reaction in Systems Containing Iron Adriamycin

The anthracycline antibiotics are being used clinically against a number of neoplasms. However, the therapeutic effects of anthracycline derivatives are severely limited by their cardiotoxic effects. Active oxygen species produced during activation of these drugs have been suggested to be responsible for the observed cardiotoxicity. Recently, it was shown that the iron–adriamycin complex causes more extensive physiological damage (i.e., lipid peroxidation, DNA damage, etc.) than activated adriamycin alone (*79,83,86*). Again, formation of active oxygen species has been proposed to account for such damaging effects. In a biological milieu, active oxygen species from activated adriamycin can arise from several enzymatic and nonenzymatic reactions. These include:

(i) reductive activation of adriamycin by NADPH-cytochrome P450 reductase, xanthine/xanthine oxidase, NADH-quinone reductase, etc., resulting in a putative semiquinone radical which, in turn, undergoes redox cycling in the presence of oxygen to give oxy radicals;

(ii) direct iron-independent reaction between the adriamycin semiquinone and hydroperoxides;

(iii) thiol-dependent reduction of Fe(III)-Adr and Fe(III)-DNA-Adr complexes;

(iv) lipid peroxidation induced by Fe(III)-ADP-Adr complex;

(v) electron-transfer reaction between Fe(III)-Adr and Adriamycin itself.

Since this chapter addresses reactions of metal-antitumor complexes, only those reactions (iii–v) involving iron and Adriamycin are considered in this section.
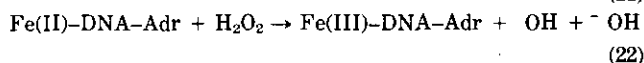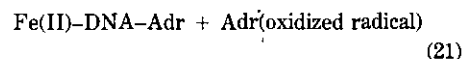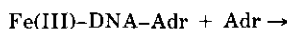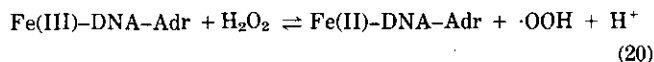
During thiol-dependent reduction of Fe(III)–Adr and Fe(III)–DNA–Adr complexes, oxygen consumption occurs, which was found to be sensitive to addition of catalase and superoxide dismutase. This suggests the involvement of superoxide and hydrogen peroxide. The following reactions can account for the observed oxygen consumption:

$$Fe(III)\text{—}Adr + RSH \rightleftharpoons Fe(II)\text{-}Adr + RS^{\cdot} + H^+ \quad (15)$$

$$Fe(II)\text{—}Adr + O_2 \rightleftharpoons Fe(III)\text{-}Adr + O_2^{\bar{}} \quad (16)$$

$$O_2^{\bar{}} + O_2^{\bar{}} + 2H^+ \rightarrow H_2O_2 + O_2 \quad (17)$$

$$RS^{\cdot} + O_2 \rightarrow RSOO^{\cdot} \quad (18)$$

Whereas direct ESR and ESR-spin trapping can be used to verify reactions (15 and (16), one can use oxygen-uptake measurements (in the presence of spin trap) to obtain evidence for reaction (18). In fact, evidence for reaction (16) has recently been shown directly by ESR (*80*). Fe(III)–Adr and Fe(III)–DNA–Adr complexes also induced extensive damage to erythrocytes and DNA in the presence of thiols (*87,88*). Involvement of hydroxyl radicals was inferred based on absence of damage in the presence of hydroxyl radical scavengers. A Fenton reaction was proposed to generate the hydroxyl radicals.

$$Fe(II)\text{—}Adr + H_2O_2 \rightleftharpoons Fe(III)\text{—}Adr + \cdot OH + {}^-OH \quad (19)$$

Evidence for hydroxyl radical production during reduction of Fe(III)–Adr and Fe(III)–DNA–Adr complexes by hydrogen peroxide was recently obtained from spin-trapping experiments (*89*). The steady-state concentrations of DMPO–OH were found to be much higher during the reduction of Fe(III)–DNA–Adr by hydrogen peroxide than of Fe(III)–Adr itself. The following reactions possibly are involved.

$$Fe(III)\text{–}DNA\text{–}Adr + H_2O_2 \rightleftharpoons Fe(II)\text{-}DNA\text{–}Adr + \cdot OOH + H^+ \quad (20)$$

$$Fe(III)\text{-}DNA\text{–}Adr + Adr \rightarrow$$
$$Fe(II)\text{–}DNA\text{–}Adr + Adr(\text{oxidized radical}) \quad (21)$$

$$Fe(II)\text{–}DNA\text{–}Adr + H_2O_2 \rightarrow Fe(III)\text{–}DNA\text{–}Adr + OH + {}^-OH \quad (22)$$

One can again monitor the initial rate of these reactions by using direct ESR and spin-trapping. The extent of DNA damage also was found to correlate with spin-trapping results. Both the reversal of DNA damage by catalase and the detection of free hydroxyl radical would seem to rule out the involvement of perferryl ion. However, with Fe(III)–ADP–Adr complex, involvement of perferryl ion has been proposed.

It was also found that the Fe(III)–ADP–Adr complex could initiate the unsaturated fatty acid decomposition which was enhanced in the presence of purified cytochrome P450 reductase and NADPH (*87*). The fatty acid decomposition was inhibited by both catalase and tocopherol. While it is conceivable that the existence of small amounts of preformed lipid hydroperoxides can explain the on-set of lipid peroxidation in the presence of Fe(III)–ADP–Adr complex [reaction (24)], the mechanism(s) leading to the enchanced lipid peroxidation in the enzymatic systems is not clear.

$$Fe(III)\text{—}ADP\text{—}Adr + LOOH \rightarrow Fe(II)\text{—}ADP\text{—}Adr + LOO^{\cdot} + H^+$$
$$LOO^{\cdot} + LH \rightarrow LOOH + L^{\cdot}$$
$$L^{\cdot} + O_2 \rightarrow LOO^{\cdot} \quad (23)$$

Fe(II)—ADP—Adr + LOOH $\rightleftharpoons$
$$Fe(III)\text{—}ADP\text{—}Adr + LO\cdot + {}^-OH \quad (24)$$
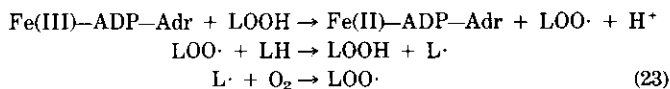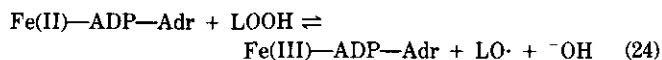
A direct electron transfer reaction between Fe(III)–Adr and excess Adr also was noted (80). The ESR spectrum of Fe(III)–Adr under anerobic conditions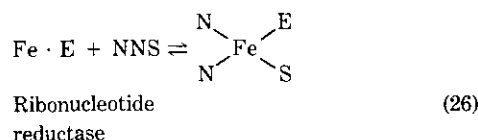 was found to decay slowly with time presumably forming the oxidized adriamycin radical (Adṙ) and Fe(II)–Adr. Upon exposure to air, the ESR signal due to the Fe(III)–Adr complex reappeared.

$$Fe(III)\text{–}Adr + Adr \rightleftharpoons Fe(II)\text{-}Adr + Adr(\text{oxidized radical}) \quad (25)$$

Reoxidation of Fe(II)Adr could occur as previously shown [reaction (16)]. Although the identity of the oxidized adriamycin radical is not known, the existence of such species has been shown previously under peroxidatic and autoxidizing conditions.
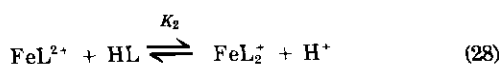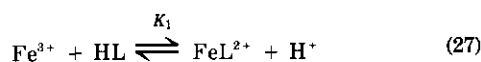
Bis(α-N-heterocyclic Carboxaldehyde Thiosemicarbazonato) Fe Complexes

An earlier section of this review described ESR studies of 2-formylpyridine thiosemicarbazonato copper which help to elucidate its behavior in Ehrlich tumor cells. Iron complexes of α-N-heterocyclic carboxaldehyde thiosemicarbazones are also cytotoxic and have antitumor properties (90). In fact, in the study of this type of ligand structure (NNS), it was thought originally that the ligand formed a ternary complex with coordinatively unsaturated iron, which was part of the active site of ribonucleotide diphosphate reductase (90).

$$Fe \cdot E + NNS \rightleftharpoons \underset{\substack{\text{Ribonucleotide} \\ \text{reductase}}}{N \diagdown \underset{N \diagup}{Fe} \diagup \overset{E}{\diagdown} S} \quad (26)$$

However, later it was suggested that the intact 2:1 ligand to iron complex reacts with the enzyme to inhibit the reduction of ribonucleotide to deoxyribonucleotides (6).

The ESR spectrum of bis(2-formylpyridine thiosemicarbazonato) Fe(III) at 77°K is a typical rhombic spectrum of a low spin complex with g values at 2.176, 2.135, and 1.998. In the formation of such complexes, a spin-state change usually occurs in the transition from the 1:1 to 2:1 ligand to metal structure.

$$Fe^{3+} + HL \overset{K_1}{\rightleftharpoons} FeL^{2+} + H^+ \quad (27)$$

$$FeL^{2+} + HL \overset{K_2}{\rightleftharpoons} FeL_2^+ + H^+ \quad (28)$$

$K_2 > K_1$ so that FeL_2^+ is formed in preference to FeL^{2+}. Given this general property and the large sta-

bility constants of $Fe(III)L_2^+$ and $Fe(II)L_2$ ($\beta_2 = 10^{26}$ and 10^{23}, respectively), both complexes are likely to exist as fully coordinated 2:1 complexes. This is in contrast to high spin Fe(III)–(Adriamycin)$_3$, which, as noted above, readily lose a ligand to become coordinately unsaturated and can form ternary adduct species.

General Comments

A common property of a number of the metal complexes described in this review is their facile redox chemistry, in which they are readily reduced by thiol compounds and oxidized by oxygen or reduced species of oxygen to produce reactive entities, including oxygen radicals and secondarily, organic free radicals. The interest in free radicals in the causation of tissue damage and in the mechanism of drug action runs deep as attested to by the subject matter of this volume. It is curious, therefore, that relatively little attention has been given to the exploration of redox-active metal complexes as drugs.

There are two features of metal complexes which make them attractive for study as metallodrugs. One can control and fine tune their redox/potential and their reactivity with oxygen. One can also study their paramagnetic forms in solution and in cells using ESR spectroscopy. Table 1 lists the redox properties of some Cu and Fe complexes of bis- and monothiosemicarbazones. It was shown that CuKTS and CuKTSM are reduced rapidly by cellular thiols (12); CuKTSM$_2$ is not and reacts in a fundamentally different way with cells (13). CuL$^+$ reacts rapidly with sulfhydryl groups (7). However, in contrast to CuKTS, Cu(I)L$^+$ is readily reoxidized to Cu(II)L in competition with the ligand substitution reaction by which thiols (RSH) react with Cu(I)L$^+$ to form Cu(I)SR. Presumably, this is because the tridentate CuL complex has an open in-plane coordination site for oxygen which the tetradentate CuKTS structure does not possess. Furthermore, the $E_{1/2}$ values for the whole series of CuL-X complexes are much more positive than for the bis thiosemicarbazone series, so that other cellular reductants may be able to reduce these structures but not CuKTS.

The monothiosemicarbazonato iron complexes also illustrate the ease with which one can manipulate redox potential (Table 1). In addition, bis(2-formylpyridine thiosemicarbazonato) Fe(II) has some kinetic stability in air though the Fe(III) complex is thermodynamically stable. Thus one expects the redox cycle of reactions (12)–(14) to be slower for FeL_2^+ than CuL$^+$. These examples point out the facility with which one can alter features of reactivity of potential metallodrugs.

Paramagnetic metallodrugs have also proven to be attractive structures for studies of mechanism of action. Usually, they have characteristic, unique ESR spectra which permit their identification in cells or model systems. For example, considering copper complexes, their geometry is usually Type II square planar or square pyramidal or blue, Type I, distorted tetrahedral.

ESR parameters $g_{\parallel}$, $A_{\parallel}$, g_{iso} and A_{iso} are easily ob-

tained and Peisach-Blumberg plots of $g_\parallel$ and $A_\parallel$ are indicative of the donor atoms bound to cupric ion (10). Well resolved lines in the $g_\perp$ region are usually the result of hyperfine structure from nitrogen donor atoms. However, interpretations from the number of well resolved lines can be ambiguous because the magnitude of $A_\perp^{Cu}$ and A^N are typically of the same order. More sophisticated techniques such as electron nuclear double resonance, low frequency S-band, and electron spin echo spectrosopy help determine nitrogen and proton hyperfine coupling constants, the number of equivalent nitrogen donor atoms, and the binding of imidazole, respectively. Molecular bonding parameters may also be calculated and are sensitive to the degree of covalency.

Upon addition of cupric complexes to cells new questions become apparent. Cells are well compartmentalized, complicated entities and knowledge of the environment of the copper complex becomes as important as obtaining ESR parameters. Studies of copper complexes in the liquid phase instead of the static (frozen) phase are necessary in order to optimize the use of cupric ion as a cellular probe. Until recently the problem with ESR data from cupric ion at room temperature was threefold. First, the sensitivity is less; second, only two ESR parameters, g^{iso} and A^{iso}, are readily extracted from fast tumbling complexes; and third, if the complex tumbles slowly, the resolution of the hyperfine structure is poorer at room temperature than in frozen solution. New instrumentation at the National Biomedical ESR Center can be used to circumvent these problems. First, the Froncisz-Hyde loop-gap resonators provide better signal to noise (91); second, a multimicrowave frequency approach allows the determination of rigid limit ESR parameters for copper from data taken at five widely varying frequencies (92); and third, although the nitrogen structure is not well resolved, the rotational correlation time, τ_R and the room temperature parameters are sensitive to the dynamics of cupric ion in, for example, cells (93). Therefore, it is anticipated that uptake of redox stable cupric complexes by cells can be used as a probe of cells much like nitroxides are used as spin labels and spin probes and that for those which react relatively slowly ($t_{1/2}$ on the order of minutes) detailed information on the nature of the reaction may be obtained under spectral conditions identical to those under which the complex is reacting with cells.

REFERENCES

1. Andrews, J. R. The Radiobiology of Human Cancer Radiotherapy. University Park Press, Baltimore, MD, 1978.
2. Hidvego, E. J., Holland, J., Streffer, C. and Beuninger, D. V. Biochemical phenomena in ionizing irradiation of cells. In: Methods in Cancer Research, Vol. 15 (H. Busch, Ed.) Academic Press, New York, 1978.
3. Prasad, K. N. Human Radiation Biology. Harper and Row, Hagerstown, MD, 1974.
4. French, F. A., and Freedlander, B. L. Chemotherapy studies on transplanted mouse tumors. Cancer Res. 21: 505–538 (1960).
5. DeConti, R. C., Toftness, B. R., Agrawal, K. C., Mead, J. A. R., Bertino, J. R., Sartorelli, A. C. and Creasey, W. A. Clinical and pharmacological studies with 5-hydroxy-2-formylpyridine thiosemicarbazone. Cancer Res. 32: 1455–1462 (1972).
6. Saryan, L. A., Ankel, E., Krishnamurti, C., and Petering, D. H. Comparative cytotoxic and biochemical effects of ligands and metal complexes of α-N-heterocyclic carboxaldehyde thiosemicarbazones. J. Med. Chem. 22: 1218–1221 (1979).
7. Saryan, L. A., Mailer, K., Krishnamurti, C., Antholine, W. and Petering, D. H. Interaction of 2-formylpyridine thiosemicarbazonato copper (II) with Ehrlich ascites tumor cells. Biochem. Pharmacol. 30: 1595–1604 (1981).
8. Antholine, W., and Taketa, F. Binding of 2-formylpyridine monothiosemicarbazonato copper II to cat and normal human hemoglobins, J. Inorg. Biochem. 16: 145–154 (1982).
9. Antholine, W., and Taketa, F. Effects of 2-formylpyridient monothiosemicarbazonato copper II on red cell components. J. Inorg. Biochem 10: 69–78 (1984).
10. Peisach, J., and Blumberg, W. E. Structural implications derived from the analysis of electron paramagnetic resonance spectra of natural and artificial copper proteins. Arch. Biochem. Biophys. 165: 691–708 (1974).
11. Antholine, W. E., Lyman, S., Petering, D. H., and Pickart, L. Formation of adducts between cupric complexes of known antitumor agents and Ehrlich ascites tumor cells, copper coordination chemistry. In: Biochemical and Inorganic Perspectives of Copper Coordination Chemistry, Adenine Press, in press.
12. Minkel, D. T., and Petering, D. H. Initial reaction of 3-ethoxy-2-oxobutyraldehyde bis(thiosemicarbazonato) copper II with ehrlich ascites tumor cells. Cancer Res. 38: 117–123 (1978).
13. Antholine, W. E., Basosi, R., Hyde, J. S., Lyman, S., and Petering, D. H. Immobile- and mobile-phase ESR spectroscopy of copper complexes: studies on biologically interesting bis(thiosemicarbazonato) copper(II) chelates. Inorg. Chem. 23: 3543–3548 (1984).
14. Kraker, A., Krezoski, S., Schneider, J. Minkel, D., and Petering, D. Reaction of 3-ethoxy-2-oxobutyraldehyde-bis (thiosemicarbazonato) Cu(II) with ehrlich cells: binding of copper to metallothionein and its relationship to cytotoxicity. J. Biol. Chem., in press.
15. Onana, P., Shaw, C. F. III, and Petering, D. H. Features of the copper-sulfur chemistry of calf liver metallothionein. Submitted for publication.
16. Warren, L. E., Flowers, L. M., and Hatfield, W. E. Electron paramagnetic resonance of bis(thiosemicarbazone)copper(II) complexes. J. Chem. Phys. 51: 1270–1271 (1969).
17. Warren, L. E., Horner, S. M., and Hatfield, W. E. Chemistry of α-diketonebis(thiosemicarbazone)copper(II) complexes. J. Am. Chem. Soc. 94: 6392–6396 (1972).
18. Campbell, M. J. M., Collis, A. J., and Grzeskowiak, R. Electron paramagnetic resonance spectrum and covalency parameters of copper-63(KTS). Bioinorg. Chem. 6: 305–311 (1976).
19. Minkel, D. T., Saryan, L. A., and Petering, D. H. Structure-function correlations in the reaction of bis(thiosemicarbazonato)copper(II) complexes with Ehrlich ascites tumor cells. Cancer Res. 38: 124–129 (1978).
20. Falchuk, K. H., Krishan, A., and Vallee, B. L. 1,10 Phenanthroline inhibition of lymphoblast cell cycles. Cancer Res. 37: 2050–2056 (1977).
21. Minkel, D. T., Dolhun, P., Calhoun, B. L., Saryan, L. A., and Petering, D. H. Zinc deficiency and growth of ehrlich ascites tumor cells. Cancer Res. 39: 2451–2456 (1979).
22. D'Aurora, V. Stern, A. M., and Sigman, D. S. Inhibition of E. coli DNA polymerase by 1,10-phenanthroline. Biochem. Biophys. Res. Commun. 78: 170–176 (1977).
23. D'Aurora, V., Stern, A. M., and Sigman, D. S. 1-10-Phenanthroline-cuprous ion complex, a potent inhibitor of DNA and RNA polymerases. Biochem. Biophys. Res. Commun. 80: 1025–1032 (1978).
24. Marshall, L. E., Graham, D. R., Reich, K. A., and Sigman, D. S. Cleavage of deoxyribonucleic acid by 1,10-phenanthroline-cu-

prous complex. Hydrogen peroxide requirement and primary and secondary structure specificity. Biochemistry 20: 244–250 (1981).

25. Downey, K. M., Que, B. G., and So, A. G. Degradation of DNA by 1,10 phenanthroline. Biochem. Biophys. Res. Commun. 93: 264–270 (1980).

26. Graham, D. R., Marshall, L. E., Reich, K. A., and Sigman, D. S. Cleavage of DNA by coordination complexes. Superoxide formation in the oxidation of 1,10-phenanthroline-cuprous complexes by oxygen-relevance to DNA-cleavage reaction. J. Am. Chem. Soc. 102: 5419–5421 (1980).

27. Kokoszka, G. F., Reimann, C. W., and Allen, H. C. The optical and magnetic spectra of copper-doped dichloro(1,10-phenanthroline) zinc. J. Phys. Chem. 71: 121–126 (1967).

28. Kwik, W. L., Ang, K. P., and Chen, G. Complexes of (2,2′-bipyridyl)copper (II) and (1,10-phenanthroline)copper(II) with some amino acids. J. Inorg. Nucl. Chem. 42: 303–313 (1980).

29. Deshpande, S. V., and Srivastava, T. S. Preparation and spectral studies of some ternary 2,2′-bipyridine and 1,10-phenanthroline copper(II) dipeptide complexes. Inorg. Chem. Acta 78: 75–80 (1983).

30. Lin, P. S., Kwock, L., and Goodchild, N. T. Copper chelator enhancement of bleomycin cytotoxicity. Cancer 46: 2360–2364 (1980).

31. Burger, R. M., Peisach, J., and Horwitz, S. B. Activated bleomycin: a transient complex of drug, iron and oxygen that degrades DNA. J. Biol. Chem. 256: 11636–11644 (1981).

32. Pettersson, R., and Vanngard, T. Electron spin resonance of Cu(II) and Ag(II) dithiocarbamates. Arkiv Kemi 17: 249–258 (1951).

33. Weeks, M. J. and Fackler, J. Single-crystal electron paramagnetic resonance studies of copper diethyldithiocarbamates. Inorg. Chem. 7: 2548–2553 (1968).

34. Gersman, H. R., and Swalen, J. D. Electron paramagnetic resonance spectra of copper complexes. J. Chem. Phys. 36: 3221 (1962).

35. Janzen, E. G. Electron spin resonance, Analytical. Chem. Ann. Rev. 46: 478R–490R (1974).

36. Antholine, W., Mailer, C., Reichling, B., and Swartz, H. M. Experimental consideration in biological ESR studies. I. Identity and origin of the 'tissue lipid signal': copper-dithiocarbamate complex. Phys. Med. Biol. 22: 840–846 (1976).

37. Yordanov, N. D., and Shopov, D. Effect of adduct formation and selfassociation on electron spin resonance spectra and electronic structure of Cu(II)diethyldithiocarbamate and di-isopropyl dithiophosphate. J. Chem. Soc. Dalton: 883–886 (1976).

38. Umezawa, H., Suhara, Y., Takita, T., and Maeda, K. Purification of bleomycins. J. Antibiotics A19: 210–215 (1966).

39. Sausville, E. A., Peisach, J., and Horwitz, S. B. Effect of chelating agents and metal ions on the degradation of DNA by bleomycin. Biochemistry 17: 2740–2746 (1978).

40. Sausville, E. A., Stein, R. W., Peisach, J., and Horwitz, S. B. Properties and products of degradation of DNA by bleomycin and iron(II). Biochemistry 17: 2746–2754 (1978).

41. Solaiman, D., Rao, E. A., Petering, D. H., Sealy, R. C., and Antholine, W. E. Chemical, biochemical and cellular properties of cooper and iron bleomycins. Int. J. Rad. Oncol. Biol. Phys. 5: 1519–1521 (1979).

42. Antholine, W. E., Solaiman, D., Saryan, L. A., and Petering, D. H. Studies on the chemical reactivity of copper bleomycin. J. Inorg. Biochem. 17: 75–94 (1982).

43. Freedman, J. H., Horwitz, S. B., and Peisach, J. Reduction of copper(II) bleomycin: a model for in vivo drug activity. Biochemistry 21: 2203–2210 (1981).

44. Iitaka, Y., Nakamura, H., Nakatani, T., Muraoka, V., Fujii, A., Takita, T., and Umezawa, H. Chemistry of bleomycin. XX. The x-ray structure determination of P-3A Cu(II) complex, a biosynthetic intermediate of bleomycin. J. Antibiot. (Tokyo) 31: 1070–1072 (1978).

45. Dabrowiak, J. C., Greenaway, F. T., Longo, W. E. and Van-Husen, M. and Crook, S. T. A spectroscopic investigation of the metal binding site of bleomycin A₂. Biochim. Biophys. Acta 517: 517–526 (1978).

46. Suguira, Y. Comparison of metal complexes between depyruvam-

ide bleomycin and bleomycin: an important effect of axial donor on metal coordination and oxygen activation. Biochem. Biophys. Res. Commun. 88: 913–918 (1979).

47. Sugiura, Y., Ishizu, K., and Miyoshi, K. Studies of metallobleomycins by electronic spectroscopy electron spin resonance spectroscopy and potentiometric titration. J. Antibiot. (Tokyo), 32: 453–461 (1979).

48. Solaiman, D., Rao, E. A., Antholine, W. and Petering, D. H. Properties of the binding of copper by bleomycin. J. Inorg. Biochem. 12: 201–220 (1980).

49. Bereman, R. D., and Winkler, M. E. A Spectral investigation of the Cu(II) complex of the antitumor compound bleomycin. J. Inorg. Biochem. 13: 95–104 (1980).

50. Shields, H., McGlumphy, C., and Hamrick, P. J., Jr. The conformation and orientation of copper(II)-bleomycin intercalated with DNA. Biochim. Biophys. Acta 697: 113–120 (1982).

51. Burger, R. M., Adler, H. D. Horwitz, S. B., Mims, W. B., and Peisach, J. Demonstration of nitrogen coordination in metal-bleomycin complexes by electron spin-echo envelope spectroscopy. Biochemistry 20: 1701–1704 (1981).

52. Antholine, W. E., Hyde, J. S., Sealy, R. C., and Petering, D. H. Structure of cupric bleomycin: nitrogen and proton couplings from EPR and electron nuclear double resonance spectroscopy. J. Biol. Chem. 259: 4437–4440 (1984).

53. Antholine, W. E., Reidy, G., Hyde, J. S., Basosi, R., and Petering, D. H. ESR Parameters of cupric bleomycin in the mobilized state. J. Biomol. Struct. Dynam. 2: 469–480 (1984).

54. Otvos, J. D., and Antholine, W. E. Cadmium as probe of transition metal interaction with bleomycin. Paper presented at 8th Meeting of International Society of Magnetic Resonance, Chicago, Illinois, Aug. 22–26, 1983, Abstract C50.

55. Burger, R. M., Peisach, J., Blumberg, W. E., and Horwitz, S. B. Ironbleomycin interactions with oxygen and oxygen analogues. J. Biol. Chem. 254: 10906–10912 (1979).

56. Burger, R. M., Horwitz, S. B., Peisach, J., and Wittenhberg, J. B. Oxygenated iron bleomycin. J. Biol. Chem. 254: 12299–12302 (1979).

57. Burger, R. M., Peisach, J., and Horwitz, S. B. Stoichiometry of DNA strand scission and aldehyde formation by bleomycin. J. Biol. Chem. 257: 8612–8614 (1982).

58. Sugiura, Y. Bleomycin-iron complexes. Electron spin resonance study, ligand effect, and implication for action mechanism. J. Am Chem. Soc. 102: 5208–5215 (1980).

59. Otsuka, M., Yoshida, M., Kobayashi, S., Ohno, M., Sugiura, Y., Takita, T., and Umezawa, H. Transition-metal binding site of bleomycin. A synthetic analogue capable of binding Fe(II) to yield an oxygen-sensitive complex. J. Am. Chem. Soc. 103: 6988–6989 (1981).

60. Sugiura, Y., Suzuki, T., Kawabe, H., Tanaka, K. and Watanabe, K. Spectroscopic studies on bleomycin-iron complexes with carbon monoxide, nitric oxide, isocyanide, azide and cyanide and comparison with iron-porphyrin complexes. Biochim. Biophys. Acta 716: 38–44 (1982).

61. Sugiura, Y., Suzuki, T., Muraoka, Y., Umezawa, Y., Takita, T., Umezawa, H. Deglyco-bleomycin-iron complexes: implications for iron-binding site and role of the sugar portion in bleomycin antibodies. J. Antibiotics 34: 1232–1236 (1981).

62. Sugiura, Y., Ishizu, K., and Miyoshi, K. Studies of metallobleomycins by electronic spectroscopy, electron spin resonance spectroscopy, and potentiometric titration. J. Antibiotics, 32: 453–461 (1979).

63. Sugiura, Y. Production of free radicals from phenol and tocopherol by bleomycin-iron(II) complex. Biochem. Biophys. Res. Commun. 87: 649–653 (1979).

64. Sugiura, Y., and Kikuchi, T. Formation of superoxide and hydroxy radicals in iron(II)-bleomycin-oxygen system. Electron spin resonance detection by spin trapping. J. Antibiot. 31: 1310–1312 (1978).

65. Peisach, J., Stern, J. O., and Blumberg, W. E. Optical and magnetic probes of the structure of cytochrome P-450's. Drug Metab. Disposit. 1: 45–61 (1973).

66. Antholine, W. E., and Petering, D. H. On the reaction of iron bleomycin with thiols and oxygen. Biochem. Biophys. Res. Com-

mun. 90: 384–389 (1979).

67. Antholine, W. E., Petering, D. H., Saryan, L. A., and Brown, C. E. Interactions among iron(II) bleomycin, Lewis bases, and DNA. Proc. Natl. Acad. Sci. (U.S.) 78: 7517–7520 (1981).

68. Oberley, L. W., and Buettner, G. R. The production of hydroxyl radical by bleomycin and iron(II). FEBS Letters. 97: 47–49 (1979).

69. Bartkowiak, A., Grzelinska, E., Bartosz, G., Zablocka, J. and Leyko, W. The crypto-OH· radical in the damage of DNA by bleomycin-Fe²⁺. Int. J. Biochem. 14: 1051–1053 (1982).

70. Takeshita, M., Grollman, A. P., Ohtsubo, E., and Ohtsubo, H. Interaction of bleomycin with DNA. Proc. Natl. Acad. Sci. (U.S.) 75: 5983–5987 (1978).

71. Antholine, W. E., and Petering, D. H. Reaction of FeBlm with DNA: Fe(II)Blm-NO. Biochem. Biophys. Res. Commun. 92: 528–533 (1979).

72. Sugiura, Y., and Ishizu, K. Metallobleomycins: electron spin resonance study on nitrosyl complex of iron(II)-bleomycin. J. Inorg. Biochem. 11: 171–180 (1979).

73. Sugiura, Y. Momeric cobalt(II)-oxygen adducts of bleomycin antibiotics in aqueous solution. A new ligand type for oxygen binding and effect of axial Lewis base. J. Am. Chem. Soc. 102: 5216–5221 (1980).

74. Sugiura, Y. Metal coordination core of bleomycin: comparison of metal complexes between bleomycin and its biosynthetic intermediate. Biochem. Biophys. Res. Commun. 87: 643–648 (1979).

75. Sugiura, Y., and Mino, Y. Nickel(III) complexes of histidine-containing tripeptides and bleomycin. Electron spin resonance characteristics and effect of axial nitrogen donors. Inorg. Chem. 18: 1336–1339 (1979).

76. Sugiura, Y., Muraoka, Y., Fujii, A., Takita, T., and Umezawa, H. Chemistry of bleomycin. XXIV. Deamido bleomycin from viewpoint of metal coordination and oxygen activation. J. Antibiotics 32: 756–758 (1979).

77. Gosalvez, M., Blanco, M. F., Vivero, C., and Valles, M. Quelamycin, a new derivative of adriamycin with several possible therapeutic advantages. Eur. J. Cancer 14: 1185–1190 (1978).

78. Young, D. M., Ward, J. M., and Pelham, J. F. Quelamycin-induced cardiotoxicity in rabbits and rats. Proc. Am. Assoc. Cancer Res. 19: 223 (1978).

79. Myers, C. E., Gianni, L., Simone, C. B., Klecker, R., and Greene, R. Oxidative destruction of erythrocyte ghost membranes catalyzed by the doxorubicin-iron complex. Biochemistry 21: 1707–1713 (1982).

80. Zweier, J. S. Reduction of O₂ by iron-adriamycin. J. Biol. Chem. 259: 6056–5068 (1984).

81. Carrington, A., and McLachlan, A. D. Introduction to Magnetic Resonance. Harper and Row, New York, 1967.

82. Gianni, L., Zweier, J. L., Levy, A., and Myers, C. E. Charac-

terization of the cycle of iron mediated electron transfer from adriamycin to molecular oxygen. Submitted for publication.

83. Eliot, H., Gianni, L., and Myers, C. Oxidative destruction of DNA by the adriamycin-iron complex. Biochemistry 23: 928–936 (1984).

84. Sinha, B. K., Muindi, J. R. F., and Myers, C. E. Correlation between hydroxyl radical generation and DNA damage by the adriamycin and 5-iminodaunomycin-iron complex. Submitted for publication.

85. Kalyanaraman, B., Sealy, R. C., and Sinha, B. K. An electron spin resonance study of the reduction of peroxides by anthracycline semiquinones. Biochim. Biophys. Acta 799: 270–275 (1984).

86. Gianni, L., Corden, B. J., and Myers, C. E. The biochemical basis of anthracycline toxicity and antitumor activity. In: Review in Biochemical Toxicology (E. Hodgson, J. R. Bend, and R. M. Philpot, Eds.), Elsevier/Holland, Vol. 5, 1983, pp. 1–82.

87. Sugioka, K., and Nakamo, M. Mechanism of phospholipid peroxidation induced by ferric ion-ADP-adriamycin co-ordination complex. Biochim. Biophys. Acta 713: 333–343 (1982).

88. Sugioka, K., Nakano, H., Nakano, M., Tero-Kubota, S., and Ikegami, Y. Generation of hydroxyl radicals during the enzymatic reductions of the Fe³⁺-ADP-phosphate-adriamycin and Fe³⁺-ADP-EDTA systems. Biochim. Biophys. Acta 753: 411–421 (1983).

89. Muindi, J. R. F., Sinha, B. K., Gianni, L., and Myers, C. E. Hydroxyl radical production and DNA damage induced by anthracycline iron complex. FEBS Letters, in press.

90. Sartorelli, A. C., Agrawal, K. C., and Moore, E. C. Mechanism of inhibitiion of ribonucleoside diphosphate reductase by α-(N)-heterocyclic aldehyde thiosemicarbazones. Biochem. Pharmacol. 20: 3119–3123 (1971).

91. Froncisz, W., and Hyde, J. S. The loop-gap resonator: a new microwave lumped circuit ESR sample structure. J. Mag. Reson. 47: 515–521 (1982).

92. Basosi, R., Antholine, W. E., Froncisz, W., and Hyde, J. S. Spinhamiltonian input parameters in the EPR analysis of liquid phase copper complexes. J. Chem. Phys. 81: 4849–4857 (1984).

93. Hyde, J. S., and Froncisz, W. The role of microwave frequency in EPR spectroscopy of copper complexes. Ann. Rev. Biophys. Bioeng. 11: 391–417 (1982).

94. Knight, J. M., Whelan, H., and Petering, D. N. Electronic substituent effects upon properties of 5-substituted 2-formylpyridine thiosemicarbazones and their metal complexes. J. Inorg. Biochem. 11: 327–338 (1979).

95. Winkelmann, D., Bermke, Y., and Petering, D. Comparative properties of the antineoplastic agent, 3-ethoxy-2-oxobutyraldehyde bis(thiosemicarbazonato) Cu(II) and related chelates: linear free energy correlations. Bioinorg. Chem. 3: 261–277 (1974).